

LIBRARY
DEPARTMENT OF NATURAL RESOURCES
GEOLOGY AND MINERAL INDUSTRIES DIVISION
OLYMPIA, WASHINGTON 98504

Preliminary Geology Of Eastern Umtanum Ridge, South-Central Washington

Fraser E. Goff

Prepared for the United States
Department of Energy
Under Contract DE-AC06-77RL01030

QE176
B4
G612p
1981
copy 2



Rockwell International

Rockwell Hanford Operations
Energy Systems Group
Richland, WA 99352



Rockwell International

Rockwell Hanford Operations
Energy Systems Group
Richland, WA 99352

DISCLAIMER

This report was prepared as an account of work sponsored by an agency of the United States Government. Neither the United States Government nor any agency thereof, nor any of their employees, makes any warranty, express or implied, or assumes any legal liability or responsibility for the accuracy, completeness, or usefulness of any information, apparatus, product, or process disclosed, or represents that its use would not infringe privately owned rights. Reference herein to any specific commercial product, process, or service by trade name, trademark, manufacturer, or otherwise, does not necessarily constitute or imply its endorsement, recommendation, or favoring by the United States Government or any agency thereof. The views and opinions of authors expressed herein do not necessarily state or reflect those of the United States Government or any agency thereof.

LIBRARY
DEPARTMENT OF NATURAL RESOURCES
GEOLOGY AND EARTH RESOURCES DIVISION
OLYMPIA, WASHINGTON 98504

PRELIMINARY GEOLOGY OF EASTERN UMTANUM RIDGE,
SOUTH-CENTRAL WASHINGTON

Fraser E. Goff
Consulting Geologist
2837 Nickel St.
Los Alamos, NM 87544

January 1981

Prepared for Rockwell Hanford Operations,
A Prime Contractor to U.S. Department of Energy,
Under Contract Number DE-AC06-77RL01030

N O T I C E

This report was prepared as an account of work sponsored by an agency of the United States Government. Neither the United States Government nor any agency thereof, nor any of their employees, makes any warranty, express or implied, or assumes any legal liability or responsibility for the accuracy, completeness, or usefulness of any information, apparatus, product or process disclosed, or represents that its use would not infringe privately owned rights. Reference herein to any specific commercial product, process, or service by trade name, trademark, manufacturer, or otherwise, does not necessarily constitute or imply its endorsement, recommendation, or favoring by the United States Government or any agency thereof. The views and opinions of authors expressed herein do not necessarily state or reflect those of the United States Government or any agency thereof.

QE176
B4
G612P
1981
copy 2

ABSTRACT

JUL 7 1981

The basalt stratigraphy and geologic structures of eastern Umtanum Ridge have been mapped and studied in detail to help assess the feasibility of nuclear waste terminal storage on the Hanford Site in southeastern Washington State. Eastern Umtanum Ridge is an asymmetric east-west-trending anticline of Columbia River basalt that plunges 5 degrees eastward into the Pasco Basin. Geologic mapping and determination of natural remanent magnetic polarity and chemical composition reveal that flows of the Pomona and Umatilla Members (Saddle Mountains Basalt), Priest Rapids and Frenchman Springs Members (Wanapum Basalt), and Grande Ronde Basalt were erupted as fairly uniform sheets. The Wahluke and Huntzinger flows (Saddle Mountains Basalt) fill a paleovalley cut into Wanapum Basalt.

Several lines of evidence show that folding of Umtanum Ridge began before Umatilla time (14 million years ago) and continued well after Pomona time (10.5 million years ago). Eventually the ridge was faulted by high-angle reverse movement on the north limb of the fold. This movement brought horizontal Wanapum lavas against overturned Grande Ronde Basalt. Shearing and fracturing associated with the thrusting and folding have produced zones of brecciated and mylonitized basalt subparallel to the strike of the fault and fold. The evidence suggests folding was caused by generally north-south compression. Many normal faults of short length and minor displacement also occur on Umtanum Ridge, indicating that similar structures are buried by glaciofluvial sediments beneath the Pasco Basin.

The Olympic-Wallowa Lineament cuts Umtanum Ridge with a north 50 degree west trend, intersecting the Umtanum anticlinal axis at the McCoy Canyon slide complex. The Olympic-Wallowa Lineament is represented in the field by short faults of minor displacement, a tight fold trending north 40 degrees west, and sheared and brecciated rock. The crest line of the fold has left-lateral displacement of 1 kilometer which may be a manifestation of the Olympic-Wallowa Lineament.

No evidence was found that indicates the artesian nature of wells and springs south of the anticline are a manifestation of the Olympic-Wallowa Lineament. Water chemistry shows the waters originate in the Vantage interbed or Frenchman Springs flows.

No evidence was found to indicate Quaternary-age movement on any structures in the map area. The basalt strata on the south limb of the Umtanum anticline display relatively little tectonic deformation since Miocene-Pliocene time. Thus, the buried south flank of Umtanum Ridge may provide an excellent location for a nuclear waste repository beneath the Hanford Site.

CONTENTS

Introduction	8
Important Note	8
Purpose.	8
Location and Physiography.	8
Methods of Investigation	10
Acknowledgments.	10
Previous Investigations.	12
 Stratigraphy	 12
Columbia River Basalt Group.	13
Saddle Mountains Basalt.	16
Wanapum Basalt	30
Grande Ronde Basalt.	32
Continuity of Individual Flows	32
The Flow-Top Breccia Problem	33
Chemical Composition	35
 Structure.	 40
Introduction	40
Umtanum Anticline.	40
Physical Character of Sheared Basalt	50
Umtanum Reverse Fault.	63
Mechanism of Folding of the Umtanum Anticline--an Interpretation	66
Age of Folding of Umtanum Ridge.	67
Eastward Extension of the Umtanum Structure.	69
Olympic-Wallowa Lineament.	69
Folding South of Umtanum Ridge	70
Normal Faults.	71
Aerial Photographic Lineaments	72
Intracanyon Structure.	72
 Landslides	 72
McCoy Canyon Slide Complex	75
Juniper Springs Slide Complex.	77

Water Quality and Geothermal Potential77
Recommendations.86
Waste Repository Site and Hydrologic Considerations.86
Seismic Considerations87
General Recommendations.88
Conclusions.89
References
Appendix90
Distribution95

FIGURES:

1. Hanford Site Map Showing Location of Mapped Area.	9
2. Pasco Basin Stratigraphic Nomenclature.14
3. Huntzinger and Wahluke Intracanyon Flows.27
4. Colonnade and Entablature of Huntzinger Flow.28
5. Pillow-Palagonite Complex29
6. Partial Columnar Stratigraphic Section.34
7. Variation of MgO Compared to TiO ₂ - Priest Rapids, Frenchman Springs, Grande Ronde Basalts36
8. Variation of MgO Compared to TiO ₂ - Saddle Mountains Basalt.37
9. Tightly Folded Monocline - North Limb of Umtanum Anticline.42
10. Pitted and Grooved Flow Top in Monocline - North Face of Umtanum Ridge.43
11. Umtanum Ridge Monocline44
12. Shear Zone.45
13. Close-Up View of Shear Zone46
14. Fractured Entablature Zone in a Flow of Grande Ronde Basalt.47
15. Crisscrossing, Tectonically Induced Fractures48
16. Intensely Folded and Fractured Umtanum Basalt Flow.49
17. Sawed Surface of Fractured and Sheared Aphyric Basalt51
18. Photomicrograph of Sample 2025B, Table 4.52
19. Photomicrograph of Sheared Basalt, Sample 2025B, Table 453

Figures (continued)

20. Extensively Brecciated and Mylonitized Aphyric Basalt, Sample C2025C, Table 454
21. Photomicrograph of Sheared Basalt, Sample 2025C, Table 455
22. Photomicrograph of Sheared Basalt, Sample C2046, Table 456
23. Photomicrograph of Sheared Basalt, Sample C2058, Table 457
24. Photomicrograph of Sheared Plagioclase Phenocryst, Sample C2069, Table 458
25. Vertical Basalt Strata Southwest of Priest Rapids Dam64
26. Sketch of Contact Relationships Adjacent to Umtanum Fault65
27. Contact Relationships between Umatilla and Priest Rapids Members.68
28. Juniper Springs Slide Complex73
29. Lineaments Visible on Areal Photographs74
30. McCoy Canyon Slide Complex.76
31. Major Slide Block, McCoy Canyon78
32. Artesian Well #1.80
33. Calculation of Depth to Vantage Interbed Horizon.85

TABLES:

1. Comparison of Average Analyses of Standard Umatilla Basalt and Umatilla Type-Locality Basalt.11
2. Distinguishing Characteristics of Grande Ronde Flows.15
3. Chemical Analyses of Samples Collected From Eastern Umtanum Ridge17
4. Descriptions of Tectonically Deformed Basalts From Eastern Umtanum Ridge59
5. Summary of X-Ray Diffraction Powder Data Sub-microscopically mylonitized Basalt Samples C2025C, C2058, C2069.61
6. Summary of X-Ray Diffraction Powder Pattern of Erionite Fibers From Sheared Basalt, Sample C2025B.62

INTRODUCTION

IMPORTANT NOTE

This report describes the geology and structure north of the Silver Dollar fault zone (along the south flank of Yakima Ridge), although Plate 1 includes all geologic mapping by the author on both Umtanum and Yakima Ridges. A summary of the structural evolution of eastern Yakima Ridge has been written by Goff and Myers (1978). All field work was performed from May 1977 to February 1978.

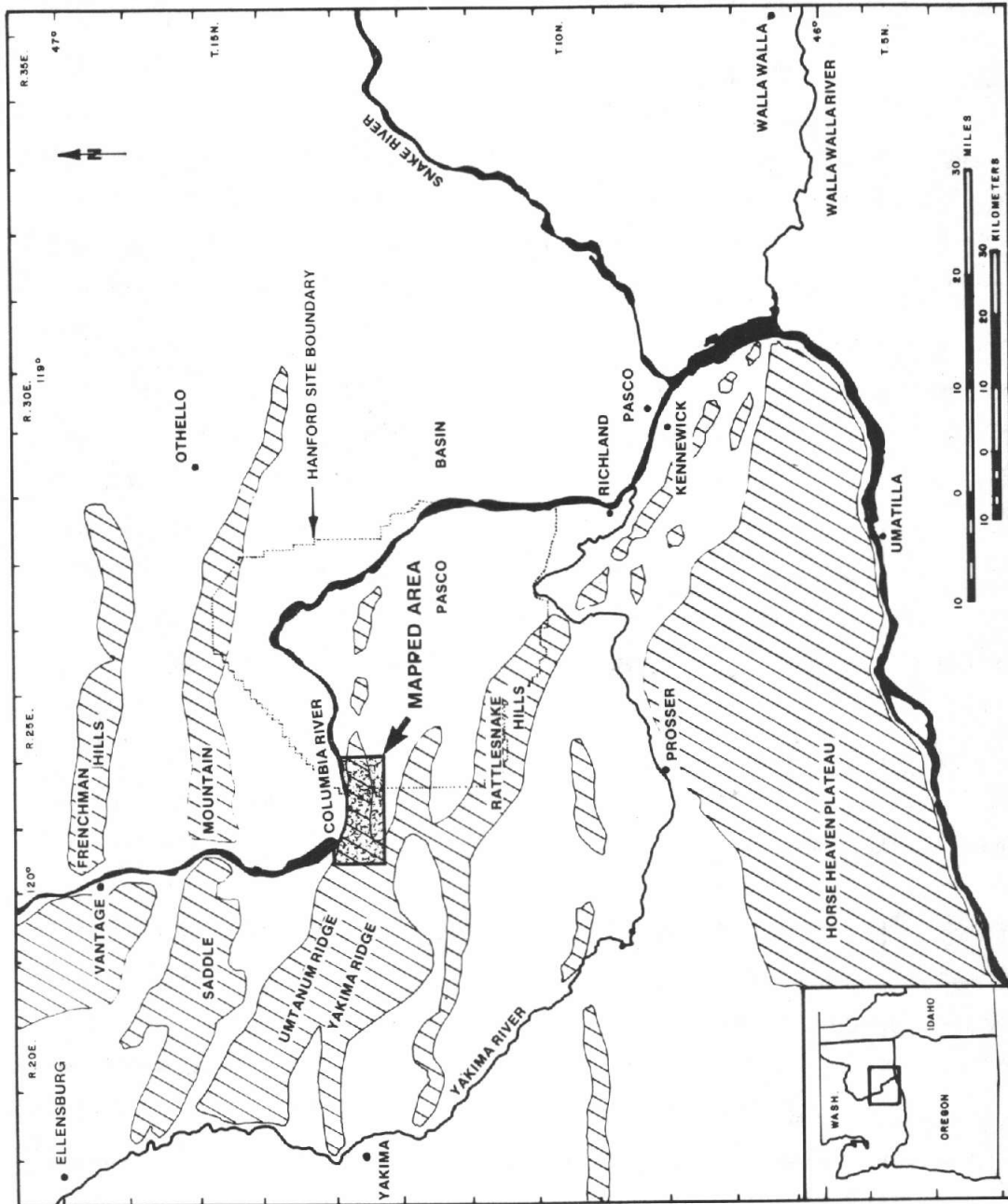
PURPOSE

Rockwell Hanford Operations (Rockwell), under contract to the U.S. Department of Energy, is assessing the feasibility of using Columbia River basalt as a medium for the final storage of commercial nuclear waste. Current emphasis is on that portion of the Columbia River basalt of the Pasco Basin which is included in the Hanford Site (Figure 1). Knowledge of the geologic relations expressed on eastern Umtanum Ridge is critical for selection and evaluation of repository sites in the Pasco Basin.

The purpose of this initial study was to map the stratigraphy and structure of Miocene basalts on eastern Umtanum Ridge, emphasizing those structures important to the hydrologic characteristics of the region. Quaternary sediments were also mapped in order to locate areas where major structures, especially faults, may have deformed young sediments. In addition, several other geologic features were investigated. These included landslides, the nature of sheared (cataclastic) basalt, flow-top breccias, and the chemistry of local groundwaters.

LOCATION AND PHYSIOGRAPHY

Umtanum Ridge lies in the mountainous desert of south-central Washington on the northwest edge of the Pasco Basin (Figure 1). The Columbia River flows eastward along the steeply dipping, north flank of the Umtanum anticline. The easternmost end of the ridge lies within the Hanford Site. The U.S. Army's Yakima Firing Center occupies the west end of the map area. Umtanum Ridge presents a panorama of barren, rocky



RCP8006-318

FIGURE 1. Hanford Site Map Showing Location of Mapped Area.

cliffs and slopes covered with sagebrush and wind-blown silt. The desert soil is locally cultivated where abundant water is available. The mapped area is traversed by state highways, but most access is by dirt road. Three months were spent in detailed mapping of 80 square kilometers and 2 months were spent in support work and preparation of this draft report.

METHODS OF INVESTIGATION

Geologic mapping was done on U.S. Geological Survey 7-1/2-minute and 15-minute quadrangle topographic maps and compiled at 7-1/2-minute (1:24,000) scale. Mapping was aided by black and white and color aerial photographs with scales of about 1:7,000 and 1:60,000, respectively.

Approximately 100 chemical analyses and natural remanent magnetic polarity measurements were made on selected samples to assist in identification of the various units of Columbia River basalt. Quantitative chemical analyses were made by standard atomic absorption techniques at a laboratory under subcontract to Rockwell. Results were reported as weight percent of oxides. All suites of samples submitted for atomic absorption analysis included two or three samples of a standard basalt (Umatilla basalt) for calibration of precision and accuracy. Comparisons of average analyses and analytical errors of standard Umatilla basalt and Umatilla type-locality basalt are listed in Table 1. Semi-quantitative analyses for barium, calcium, and titanium were made on an energy-dispersive X-ray fluorescence unit. Natural remanent magnetic polarities were obtained using a portable flux gate magnetometer (Calex Model 70). Samples of breccia and mylonite from mapped shear zones were studied using standard petrographic and X-ray diffraction powder techniques. A stratigraphic section through the Grande Ronde Basalt was measured with tape and compass. Spring and well water samples were collected according to the methods of Thompson (1975) and chemically analyzed by a laboratory under subcontract to Rockwell.

ACKNOWLEDGMENTS

I gratefully appreciate the experienced advice and support of Dr. C. W. Myers, Mr. J. N. Gardner, Mr. K. R. Fecht, and Ms. M. G. Jones. Mssrs. M. Neese and R. D. Landon, and Ms. A. Marke1 aided with various

TABLE 1. Comparison of Average Analyses of Standard Umatilla Basalt and Umatilla Type-Locality Basalt. (Error reported by this study is average relative error; analyses reported are as mean percents.)

Chemicals Analyzed	Average of 14 Umatilla Standard	Umatilla Standard Analyses*
SiO ₂	52.4 ± 0.6	52.54
Al ₂ O ₃	13.8 ± 0.4	13.79
FeO	12.9 ± 0.3	13.73
MgO	2.89 ± 0.08	2.95
CaO	6.37 ± 0.15	6.40
Na ₂ O	3.23 ± 0.10	3.20
K ₂ O	2.55 ± 0.17	2.52
MnO	0.22 ± 0.01	0.19
TiO ₂	2.91 ± 0.14	2.76
P ₂ O ₅	0.94 ± 0.10	0.90

*This report.

**Additon and Seil, 1979.

aspects of geologic mapping, water sampling, sample preparation, and magnetic determinations. Ms. K. Ferguson and Dr. M. W. Grutzcek arranged for water analyses. Mr. D. H. Parks assisted with petrographic photography. Dr. A. C. Waters, Dr. D. A. Swanson, and Mr. S. Farooqui offered valuable advice. Dr. S. P. Reidel reviewed the manuscript.

PREVIOUS INVESTIGATIONS

The regional geology of the Pasco Basin vicinity was compiled and described by Grolier and Bingham (1965) and by Newcomb (1970). Umtanum Ridge appears on Newcomb's map, but because of the scale of this compilation, the geology is highly generalized. A reconnaissance geologic map (1:100,000 scale) was prepared by Washington Public Power Supply System, Inc. (WPPSS, 1974). The structural geology presented on that map is essentially in agreement with the findings of this study, but identification of basalt members and delineation of their extent are locally in disagreement. A reconnaissance report on the geology of the McCoy Canyon area was prepared by Converse, Davis and Associates (1970) and their conclusions differ from those of this report. Details of surface and subsurface geology were interpreted by Mackin (1955) in a report for the Public Utility District No. 2 of Grant County, Washington regarding construction of Priest Rapids Dam. In spite of minor misidentification of some basalt members, the results of that report are here referred to repeatedly. Geologic studies conducted by the Atlantic Richfield Hanford Company in the Pasco Basin and Columbia Plateau region were summarized in ARH-ST-137 (1976).

STRATIGRAPHY

The dominant lithology of the area is basalt of the Columbia River Basalt Group that is covered by various types of Quaternary sediments. These young deposits are primarily alluvium and older gravels associated with Cold Creek and the Columbia River. A large fan of glaciofluvial gravels and sediments spreads southeastward from the Columbia River around the eastward-plunging end of the Umtanum anticline. Recent

Columbia River gravels are easily distinguished from local gravels by the occurrence of granitic and metamorphic cobbles in the former, which are absent in sediments of Cold Creek Valley and similar valleys. The southeastern slopes of the ridge, which are primarily eroded dip-slopes, are coated with a veneer of loess. Landslides appear on steep slopes and/or structurally weakened slopes.

The stratigraphic units of the map area are correlated with units previously defined in the Pasco Basin by their stratigraphic position, remanent magnetic polarity, and whole-rock chemical composition, as based on data reported by Wright and Others (1973) and Ledgerwood and Others (1973). Stratigraphic nomenclature of the Pasco Basin is given in Figure 2.

COLUMBIA RIVER BASALT GROUP

The Columbia River Basalt Group is very difficult to map at a member or flow level of detail without positive identification by whole-rock chemical composition. Field criteria, such as abundance of phenocrysts, stratigraphic position, interbed characteristics, and primary flow features (e.g., columns, pillows, etc.), generally distinguish the three basalt formations and many members from one another. However, these characteristics vary, especially over a large area, but also within the map area. Positive identification of flows from hand samples of isolated outcrops is difficult, particularly where identification involves comparisons distinguishing Pomona from Huntzinger, Umatilla from Wahluke, and among Priest Rapids, aphyric Frenchman Springs, and upper Grande Ronde Basalt. In general, the Columbia River basalt is composed of tholeiitic lavas having both normative quartz and hypersthene and consisting of plagioclase, pyroxene, opaques, glass, and olivine.

Detailed field descriptions of individual units are given in the Appendix. Distinctive characteristics are described below and in Table 2. The chemical characteristics are described in a following section. See Table 1 for analyses of standards.

PASCO BASIN STRATIGRAPHIC NOMENCLATURE

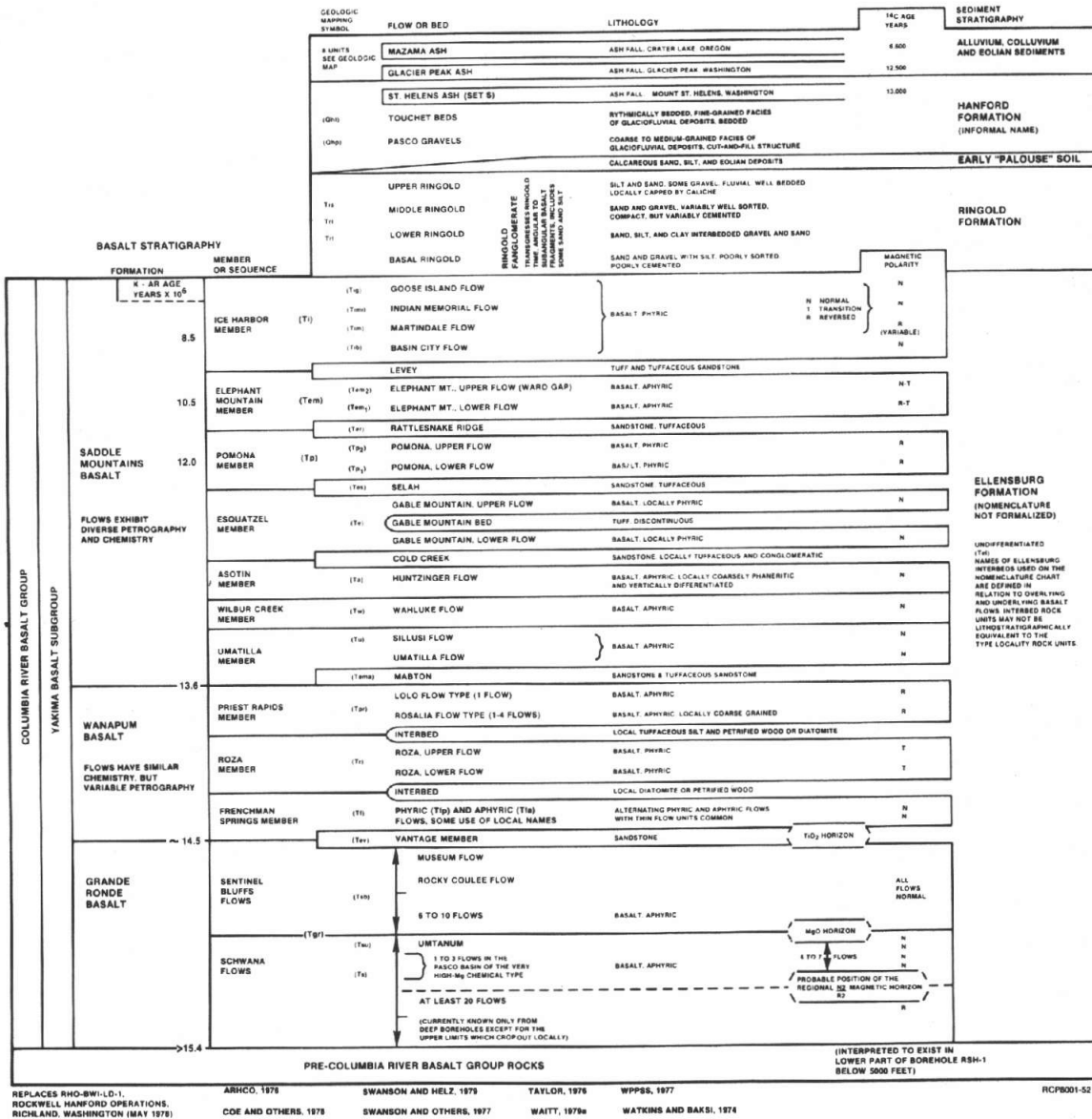


FIGURE 2. Pasco Basin Stratigraphic Nomenclature.

TABLE 2. Distinguishing Characteristics of Grande Ronde Flows.

<u>Flow 1 (Museum?):</u>	This flow has a diktytaxitic texture, with tiny vesicles and abundant microphenocrysts.
<u>Flow 2 (Rocky Coulee?):</u>	This flow is dense, black, glassy, and aphyric; its appearance is in sharp contrast to the above flow.
<u>Flow 5 (Unnamed):</u>	This flow is distinctive because of its relatively coarse, microporphyritic, and slightly diktytaxitic texture and thin, fanning entablature columns.
<u>Flow 8 (Unnamed):</u>	This flow has a very distinctive diktytaxitic texture, scattered vesicle cylinders, and vesicle sheets (Goff, 1976 and 1977).
<u>Flow 9 (Unnamed):</u>	This flow is relatively thick (about 60 meters) has a 12- to 15-meter-thick flow-top breccia, and consists of two separate flow units.
<u>MgO Horizon:</u>	Flows below this horizon contain less magnesium oxide than the flows described above.
<u>Flow 10 (Umtanum):</u>	The Umtanum flow is over 90 meters thick in the McCoy Canyon measured section and contains a flow-top breccia which is locally more than 50 meters thick. This flow has a thick entablature with fanning columns and a relatively thin colonnade.

SADDLE MOUNTAINS BASALT

The Saddle Mountains Basalt consists of sheet flows of the Pomona and Umatilla Members and the intracanyon Asotin (Huntzinger) and Wilbur Creek (Wahluke) Members.

The Pomona flow is best exposed in the core of the Cold Creek syncline and is characterized by thin, fanning columns, conspicuous olivine, sieve-textured plagioclase phenocrysts, and reverse natural remanent magnetic polarity. Zones of pillowing in the Pomona were mapped in the Cold Creek syncline axis. The Pomona overlies rare outcrops of volcanoclastic sediment and rhyolite tuff of the Selah interbed (Ellensburg Formation) on the south flank of Umtanum Ridge. On the north flank, the tuff forms an extensive sheet several meters thick. Locally, the tuff shows additional welding by the overlying Pomona (Schmincke, 1967) to a dark grey, perlitic glass. This relationship can be seen in the South 1/2, Section 24, Township 13 North, Range 24 East (abbreviated S 1/2 Sec. 24, T13N, R24E). Chemical analyses of welded and unwelded tuff are given in Table 3 (Samples C2004s and C2109, respectively. Also member abbreviations are given in Figure 2, Pasco Basin Stratigraphic Nomenclature).

Intracanyon flows of the Huntzinger and Wahluke basalts fill a paleovalley that was cut by an ancient stream through flows of Priest Rapids and Roza or "Roza-like" basalts (Figure 3). The Huntzinger flow has variable appearance in hand sample as discussed by Ward (1976). Some samples are glassy and porphyritic, but others are distinctively spotted and have a diabasic texture. The Huntzinger contains small phenocrysts of olivine. Two outcrops of the Huntzinger flow on the south flank of Umtanum Ridge and one outcrop below Priest Rapids Dam have thick colonnade columns (Figure 4). Therefore, the normal, natural remanent magnetic polarity and the intracanyon setting are the principal means of distinguishing Huntzinger from Pomona.

Eroded remnants of the Wahluke flow extend southwestward from Emerson Nipple on Umtanum Ridge to a small mesa on the crest of Yakima Ridge. Primary features of the Wahluke flow are poorly exposed, but they resemble those of the Umatilla. Hand samples are black and glassy,

TABLE 3. Chemical Analyses of Samples Collected from Eastern Umtanum Ridge.

SAMPLE NUMBER	C2003a	C2003b	C2004p	C2004s	C2005	C2007	C2010	C2012	C2018a	C2018b
LOCATION	Sec. 13 T13N R24E	Sec. 13 T13N R24E	Sec. 24 T13N R24E	Sec. T13N R24E	Sec. 13 T13N R24E	Sec. 13 T13N R24E	Sec. 13 T13N R24E	Sec. 13 T13N R24E	Sec. 21 T13N R24E	Sec. 21 T13N R24E
MEMBER	Tpr	Tpr	Tp	Tel	Tfup	Tu	Tfu	Tpr	Tpr	Tpr
REMANENT MAGNETIC POLARITY	R	R	R	-	N	N	N	N	N	N
ATOMIC ABSORPTION ANALYSES										
SiO ₂	48.9	49.3	49.8	64.9	49.2	52.1	48.3	47.8	49.8	49.3
Al ₂ O ₃	14.4	13.4	14.8	13.0	14.2	13.3	13.3	13.6	14.7	14.1
FeO	15.0	15.0	9.66	2.03	13.5	13.0	15.2	13.3	14.4	14.1
MgO	4.35	4.67	6.27	0.57	4.43	2.60	3.94	4.67	5.05	4.96
CaO	8.37	8.40	11.4	1.07	8.49	6.30	7.67	8.90	8.66	8.88
Na ₂ O	2.62	2.58	2.39	1.94	2.79	2.92	2.74	2.73	2.75	2.82
K ₂ O	0.99	0.96	0.65	4.43	1.06	2.22	1.28	1.13	1.14	1.12
MnO	0.23	0.23	0.17	0.05	0.19	0.20	0.21	0.21	0.22	0.21
TiO ₂	3.58	3.50	1.52	0.34	2.84	2.78	3.01	2.92	3.08	2.97
P ₂ O ₅	0.62	0.73	0.29	0.14	0.58	0.84	0.68	0.82	0.75	0.73
VOLATILES	1.98	2.19	2.17	5.95	1.67	2.18	1.98	1.92	1.19	1.60
TOTAL	101.0	101.0	99.1	94.5	99.0	98.4	98.3	98.0	101.7	100.8
Ba (ppm)	650	650	670	572	483	3400	620	530	620	600

Table 3 (continued)

SAMPLE NUMBER	C2025	C2029a	C2029b	C2044	C2048a	C2048b	C2049a	C2049b	C2050	C2055b
LOCATION	Sec. 16 T13N R24E	Sec. 16 T13N R24E	Sec. 16 T13N R24E	Sec. 19 NE 1/4 T13N R24E	Sec. 13 T13N R23E	Sec. 13 T13N R23E	Sec. 30 T13N R24E	Sec. 30 T13N R24E	Sec. 28 T13N R24E	Sec. 14 T13N R24E
MEMBER	Tfu	Tfup	Tfup	Tw	Tfu	Tfu	Tpr	Tpr	Tp	Tfu
REMANENT MAGNETIC POLARITY	N	N	N	N	N	N	N	N?	R	N
ATOMIC ABSORPTION ANALYSES										
SiO ₂	49.4	49.0	49.8	51.0	49.5	50.7	49.1	48.6	51.4	50.0
Al ₂ O ₃	13.0	12.7	12.7	15.8	12.7	13.3	12.8	11.8	14.9	12.5
FeO	14.6	15.1	15.6	11.3	15.0	14.3	13.6	14.5	9.18	14.1
MgO	4.04	4.20	4.16	5.44	4.33	4.37	5.39	5.47	6.22	4.56
CaO	7.90	7.66	7.66	8.62	7.72	7.54	8.14	8.33	11.1	7.65
Na ₂ O	2.43	2.82	2.76	2.66	3.04	3.01	2.71	2.78	2.47	2.90
K ₂ O	1.23	1.19	1.19	1.40	1.29	1.34	1.04	1.09	0.72	1.31
MnO	0.23	0.23	0.24	0.16	0.21	0.23	0.22	0.22	0.16	0.22
TiO ₂	1.81	3.10	3.07	1.80	3.14	2.97	2.99	3.16	1.73	2.96
P ₂ O ₅	0.75	0.71	0.74	0.43	0.62	0.60	0.69	0.73	0.28	0.60
VOLATILES	2.83	1.68	0.89	1.18	1.49	1.57	2.08	1.77	2.19	1.79
TOTAL	99.2	98.4	98.8	99.8	9.0	99.9	98.9	98.8	98.5	100.4
Ba (ppm)	550	630	640	106	1000	850	800	730	510	730

Table 3 (continued)

SAMPLE NUMBER	C2059	C2060	C2061	C2062	C2063	C2067a	C2067b	C2068	C2069	C2071
LOCATION	Sec. 12 T13N R23E	Sec. 24 T13N R23E	Sec. 24 T13N R23E	Sec. 24 T13N R23E	Sec. 24 T13N R23E	Sec. 32 T13N R24E				
MEMBER	Tsb	Tsb	Tsb	Tsb	Tsb	Ta	Ta	Tfup	Tpr	Tp
REMANENT MAGNETIC POLARITY	N	N	N	N	N	N	N	N	R	R
ATOMIC ABSORPTION ANALYSES										
SiO ₂	53.7	53.6	51.2	51.3	52.3	51.2	52.2	47.9	49.1	50.4
Al ₂ O ₃	14.2	14.4	14.6	14.3	14.2	15.1	14.7	13.8	13.3	13.9
FeO	12.7	12.2	12.0	11.7	11.4	11.3	11.3	14.1	15.1	10.4
MgO	4.93	4.67	4.96	4.93	4.55	6.15	6.65	4.56	4.28	6.41
CaO	8.25	8.08	9.23	9.04	8.40	9.70	9.31	8.13	8.27	10.5
Na ₂ O	3.29	3.11	3.18	3.11	3.04	2.59	2.57	2.68	2.81	2.28
K ₂ O	1.26	1.27	1.41	1.10	1.32	1.48	1.27	1.42	1.24	0.60
MnO	0.22	0.21	0.20	0.19	0.19	0.07	0.17	0.20	0.24	0.19
TiO ₂	1.95	1.86	1.92	1.93	1.93	2.03	1.73	2.88	3.36	1.64
P ₂ O ₅	0.49	0.51	0.51	0.53	0.57	0.56	0.55	0.81	0.96	0.27
VOLATILES	1.00	1.50	2.20	2.29	2.39	1.29	1.79	2.55	1.30	1.62
TOTAL	102.0	101.4	101.4	100.4	100.3	101.6	101.7	99.0	100.0	98.2
Ba (ppm)	720	430	440	420	680	875	1040	390	793	250

Table 3 (continued)

SAMPLE NUMBER	C2072	C2073	C2075	C2076	C2077	C2078	C2079	C2080	C2081	C2083
LOCATION	Sec. 32 T13N R24E	Sec. 31 T13N R24E	Sec. 36 T13N R23E	Sec. 3 T13N R23E	Sec. 34 T12N R24E	Sec. 34 T13N R23E	Sec. 27 T13N R23E	Sec. 27 T13N R23E	Sec. 27 T13N R23E	Sec. 24 T13N R23E
MEMBER	Tp	Tu	Tpr	Tpr	Tem	Tw	Tpr	Tfup	Tfu	Tw
REMANENT MAGNETIC POLARITY	R	N	R	R	T	N	R	N	N	R?
ATOMIC ABSORPTION ANALYSES										
SiO ₂	50.0	51.1	48.8	48.8	49.1	53.1	47.7	48.5	50.2	50.9
Al ₂ O ₃	14.6	14.5	15.2	14.5	13.7	14.6	13.4	14.1	13.3	15.1
FeO	11.6	12.6	13.7	14.4	14.9	11.3	12.8	13.7	14.4	11.6
MgO	5.35	3.07	5.68	5.78	3.93	4.20	3.97	4.59	4.22	5.11
CaO	9.42	6.42	9.16	9.18	8.39	8.71	8.70	8.58	8.17	8.60
Na ₂ O	2.44	3.18	2.87	2.77	2.46	2.75	2.73	2.75	2.69	2.61
K ₂ O	0.45	2.66	1.04	1.11	0.96	1.66	0.79	1.16	1.33	1.31
MnO	0.16	0.22	0.25	0.26	0.23	0.18	0.20	0.21	0.23	0.18
TiO ₂	1.66	2.74	2.24	3.26	3.38	1.92	3.87	3.08	3.10	1.90
P ₂ O ₅	0.46	0.93	0.90	0.90	0.70	0.65	0.87	0.76	0.77	0.61
VOLATILES	5.58	2.19	0.49	0.79	2.49	2.59	6.08	2.84	3.29	2.87
TOTAL	101.3	99.6	101.3	101.7	100.2	101.9	101.2	100.3	101.7	100.8
Ba (ppm)	400	4600	1200?	1070?	1490?	1070	460	740	750	820

Table 3 (continued)

SAMPLE NUMBER	C2084a	C2084b	C2088	C2089	C2090	C2091a	C2091b	C2092	C2093	C2094
LOCATION	Sec. 25 T13N R23E	Sec. 25 T13N R23E	Sec. 23 T13N R23E	Sec. 26 T13N R23E	Sec. 26 T13N R23E	Sec. 26 T13N R23E	Sec. 26 T13N R23E	Sec. 30 T13N R24E	Sec. 24 T13N R23E	Sec. 24 T13N R23E
MEMBER	Tfu	Tfu	Tfu	Tfup	Tfup	Tfup	Tfup	Tpr	Tpr	Ta
REMANENT MAGNETIC POLARITY	N	N	N	N	N	N	N	R	N	N
ATOMIC ABSORPTION ANALYSES										
SiO ₂	50.9	50.3	51.1	49.5	48.3	50.4	49.8	48.0	48.8	50.0
Al ₂ O ₃	13.7	13.5	14.6	14.0	14.3	13.7	13.3	13.8	13.9	16.2
FeO	14.8	14.4	13.7	14.2	13.8	14.8	14.5	14.3	14.9	11.4
MgO	4.36	4.30	3.56	4.33	4.32	4.34	4.17	5.55	4.48	5.99
CaO	8.22	7.95	7.64	8.45	8.04	8.34	8.35	9.03	8.40	9.56
Na ₂ O	2.77	2.78	3.12	2.84	2.91	2.68	2.86	2.84	2.91	2.45
K ₂ O	1.39	1.41	1.42	1.31	1.28	1.29	1.59	1.35	1.44	1.30
MnO	0.24	0.23	0.18	0.21	0.22	0.23	0.21	0.24	0.24	0.19
TiO ₂	3.26	3.15	3.12	2.99	2.92	2.93	2.79	3.01	2.94	1.73
P ₂ O ₅	0.74	0.78	0.74	0.72	0.74	0.74	0.82	0.99	0.78	0.56
VOLATILES	0.97	2.28	2.20	1.67	1.79	2.39	1.58	1.29	2.20	2.29
TOTAL	101.4	101.1	101.8	100.2	98.6	101.8	100.0	100.4	101.0	101.7
Ba (ppm)	900	940	1000	840	770	850	550	550	650	670

Table 3 (continued)

SAMPLE NUMBER	C2095a	C2095b	C2096	C2097	C2098a	C2098b	C2099a	C2099b	C2100	C2101
LOCATION	Sec. 13 T13N R23E	Sec. 13 T13N R23E	Sec. 23 T14N R23E	Sec. 17 T13N R24E	Sec. 2 T12N R23E	Sec. 2 T12N R23E	Sec. 17 T13N R24E	Sec. 17 T13N R24E	Sec. 17 T13N R24E	Sec. 17 T13N R24E
MEMBER	Tpr	Tpr	Tpr	Tfup	Tu	Tu	Ts	Ts	Ts	Ts
REMANENT MAGNETIC POLARITY	N	R	N	N	N	N	N	N	N	N
ATOMIC ABSORPTION ANALYSIS										
SiO ₂	47.8	48.1	48.8	48.9	50.6	51.9	53.3	54.1	55.4	57.0
Al ₂ O ₃	13.0	13.3	14.1	13.6	14.0	13.5	13.8	13.6	12.9	12.6
FeO	15.5	15.4	14.2	14.9	12.8	12.8	12.9	12.8	13.1	12.0
MgO	4.58	4.54	4.42	4.09	3.05	3.05	3.60	3.50	3.54	3.34
CaO	8.61	8.53	8.28	8.25	6.77	6.85	7.15	7.087	7.18	6.86
Na ₂ O	2.70	2.63	2.96	3.01	3.10	3.08	3.06	3.04	3.04	2.90
K ₂ O	1.53	1.53	1.45	1.43	2.61	2.73	1.53	1.51	1.46	1.89
MnO	0.26	0.25	0.23	0.25	0.23	0.23	0.22	0.22	0.22	0.21
TiO ₂	3.47	3.24	2.99	3.10	3.05	2.83	2.27	2.27	2.23	2.19
P ₂ O ₅	0.96	0.99	0.77	0.91	1.01	1.07	0.58	0.53	0.58	0.57
VOLATILES	2.20	2.16	1.20	1.50	2.07	1.69	1.29	1.19	1.00	1.49
TOTAL	100.6	100.7	99.4	99.9	99.3	99.7	99.7	99.8	100.7	101.1
Ba (ppm)	670	630	570	490	2800	3500	500	510	480	530

Table 3 (continued)

SAMPLE NUMBER	C2101	C2103	C2105a	C2105b	C2106	C2107	C2108	C2109	C2110	C2111
LOCATION	Sec. 17 T13N R24E	Sec. 15 T13N R24E	Sec. 14 T13N R23E	Sec. 14 T13N R23E	Sec. 22 T13N R23E	Sec. 2 T13N R23E	Sec. 3 T13N R23E	Sec. 3 T14N R23E	Sec. 33 T14N R23E	Sec. 33 T14N R23E
MEMBER	Tsu	Tsb	Tsb	Tsb	Tfup	Tpr	Tpr	Te1	Tfup	Tsb
REMANENT MAGNETIC POLARITY	N	N	N	N	R?	N	N	-	N	N
ATOMIC ABSORPTION ANALYSES										
SiO ₂	55.7	52.9	51.4	51.6	51.7	49.0	49.6	70.2	53.0	55.8
Al ₂ O ₃	13.2	13.4	14.7	16.1	12.8	12.9	13.2	11.4	13.1	13.9
FeO	12.9	11.0	9.62	9.73	12.6	12.0	13.2	1.93	13.4	9.32
MgO	3.50	4.83	4.93	4.86	4.20	4.80	5.26	0.96	3.89	4.55
CaO	7.07	8.94	8.42	8.45	8.51	9.35	8.95	1.04	8.22	8.39
Na ₂ O	3.12	2.77	2.89	2.88	2.49	2.30	2.48	1.12	2.74	2.60
K ₂ O	1.49	1.38	1.35	1.35	1.07	0.76	1.05	4.00	1.18	1.07
MnO	0.22	0.21	0.19	0.19	0.24	0.21	0.26	0.04	0.23	0.17
TiO ₂	2.36	1.81	2.00	1.88	2.75	2.76	3.08	0.38	3.00	1.62
P ₂ O ₅	0.56	0.52	0.49	0.47	0.74	0.87	0.89	0.15	0.80	0.48
VOLATILES	1.65	2.46	2.52	2.57	3.57	4.76	2.17	8.57	2.24	3.28
TOTAL	101.8	100.2	98.5	100.1	100.7	99.7	100.1	99.8	101.8	101.2
Ba (ppm)	910	500	490	570	470	660	560	650	570	790

Table 3 (continued)

SAMPLE NUMBER	C2112	C2113	C2113b	C2114	C2115	C2116	C2117	C2118	C21119	C2120
LOCATION	Sec. 33 T14N R23E	Sec. 33 T14N R23E	Sec. 3 T13N R23E	Sec. 10 T13N R23E	Sec. 10 T13N R23E	Sec. 10 T13N R23E	Sec. 10 T13N R23E	Sec. 24 T13N R23E	Sec. 24 T13N R23E	Sec. 30 T13N R24E
MEMBER	Tp	Tpr	Tsu	Tsb	Tsu	Tsb	Tfu	Tpr	Tpr	Tu
REMANENT MAGNETIC POLARITY	R	R	N	N	N	-	N	N	N?	-
ATOMIC ABSORPTION ANALYSES										
SiO ₂	53.8	47.7	52.5	54.0	52.9	52.8	50.7	46.1	47.3	52.1
Al ₂ O ₃	14.3	13.2	13.2	13.7	13.1	13.2	13.7	13.7	12.4	12.7
FeO	9.66	13.5	3.54	11.8	13.0	12.1	11.5	14.7	15.9	13.1
MgO	6.75	5.25	7.04	3.34	3.64	3.49	4.88	3.79	4.68	2.82
CaO	10.8	9.50	2.83	2.85	3.16	2.81	2.50	2.55	2.68	2.91
Na ₂ O	2.14	2.30	1.58	1.67	1.55	1.24	0.89	0.73	1.17	2.23
K ₂ O	0.79	0.88	0.22	0.19	0.23	0.23	0.24	0.24	0.27	0.21
MnO	0.20	0.25	2.04	1.83	2.09	2.24	1.84	3.19	3.44	2.86
TiO ₂	1.72	3.13	0.54	0.49	0.57	0.84	0.50	0.91	1.01	1.00
P ₂ O ₅	0.42									
VOLATILES	1.09	2.39	1.68	1.67	3.05	1.99	2.57	3.96	1.10	2.46
TOTAL	101.7	99.0	98.3	98.4	100.7	98.5	98.4	98.8	98.3	99.1
Ba (ppm)	245	550	540	620	700	520	670	390	3060	730

Table 3 (continued)

SAMPLE NUMBER	C2121	C2122	C2123	C2124	C2125	C2126	C2127	C2128	C2129	C2130
LOCATION	Sec. 13 T13N R24E	Sec. 11 T13N R23E	Sec. 11 T13N R23E	Sec. 13 T13N R24E	Sec. 1 T13N R24E					
MEMBER	Tfu	Tsb	Tsu	Tfu	Ts	Tsb	Tsb	Tsb	Tsb	Tsb
REMANENT MAGNETIC POLARITY	N	N	-	N	N	N	N	N	N	N
ATOMIC ABSORPTION ANALYSES										
SiO ₂	48.8	50.7	51.2	49.7	53.0	52.6	52.9	52.8	52.4	52.2
Al ₂ O ₃	12.6	13.3	12.9	13.3	13.4	13.9	16.3?	16.3?	15.8	15.9
FeO	14.4	12.6	12.5	14.4	11.9	11.1	10.7	11.0	11.5	11.3
MgO	4.31	4.44	3.34	4.42	3.44	4.60	4.94	4.33	4.61	4.98
CaO	2.71	7.66	6.65	8.12	6.94	8.01	8.64	8.20	8.43	8.98
Na ₂ O	1.38	2.48	2.64	2.70	3.03	2.76	2.77	2.86	2.81	2.78
K ₂ O	0.27	0.91	1.06	1.29	1.61	1.26	1.15	1.38	1.17	1.00
MnO	3.05	0.22	0.20	0.24	0.20	0.20	0.20	0.19	0.21	0.19
TiO ₂	0.84	1.84	2.12	2.77	2.01	1.67	1.60	1.77	1.80	1.79
P ₂ O ₅		0.53	0.60	0.78	0.56	0.52	0.47	0.53	0.57	0.46
VOLATILES	1.96	3.46	4.86	1.19	2.40	2.42	1.79	2.08	1.74	1.88
TOTAL	98.5	98.1	98.1	98.9	98.5	99.0	101.5	101.4	101.0	101.5
Ba (ppm)	730	210	390	330	680	100?	460	560	330	270

Table 3 (continued)

SAMPLE NUMBER	C2131	C2132	C2133	C2134	C2135	C2140	C2143	C2145	C2146	C2147
LOCATION	Sec. 1 T13N R24E	Sec. 2 T13N R23E	Sec. 30 T13N R24E	Sec. 7 T13N R24E	Sec. 12 T13N R23E	Sec. 12 T13N R23E				
MEMBER	Tsb	Tsb	Tsb	Tsb	Tsu	Ta	Tp	Tsu	Tsb	Tsu
REMANENT MAGNETIC POLARITY	N	N	N	N	-	N	R	N	N	N
ATOMIC ABSORPTION ANALYSES										
SiO ₂	51.9	52.3	51.3	51.2	53.7	50.9	48.7	52.6	50.8	51.6
Al ₂ O ₃	15.4	15.9	15.8	16.2	16.6	17.0	15.1	14.7	14.9	14.8
FeO	12.0	12.0	11.8	12.2	11.5	10.8	10.6	12.5	12.2	12.0
MgO	4.49	4.77	5.14	4.70	3.51	6.43	6.73	3.50	4.64	3.60
CaO	8.41	8.14	8.50	7.86	6.82	9.94	10.7	7.33	8.52	7.42
Na ₂ O	2.78	2.82	2.67	3.01	3.07	2.42	2.37	3.14	3.04	2.94
K ₂ O	1.16	1.07	0.94	1.24	1.73	1.19	0.79	1.70	1.27	1.80
MnO	0.20	0.21	0.21	0.22	0.23	0.18	0.20	0.23	0.22	0.24
TiO ₂	1.94	1.85	.74	1.78	2.29	1.30	1.43	1.64	1.82	1.63
P ₂ O ₅	0.50	0.55	0.50	0.53	0.63	0.48	0.38	0.51	0.43	0.55
VOLATILES	1.79	2.38	2.57	2.34	1.56	1.10	1.08	1.28	0.40	1.68
TOTAL	100.6	102.0	101.2	101.3	101.4	101.7	98.1	99.1	98.2	98.3
Ba (ppm)	480	370	380	640	920	548	326	515	345	431

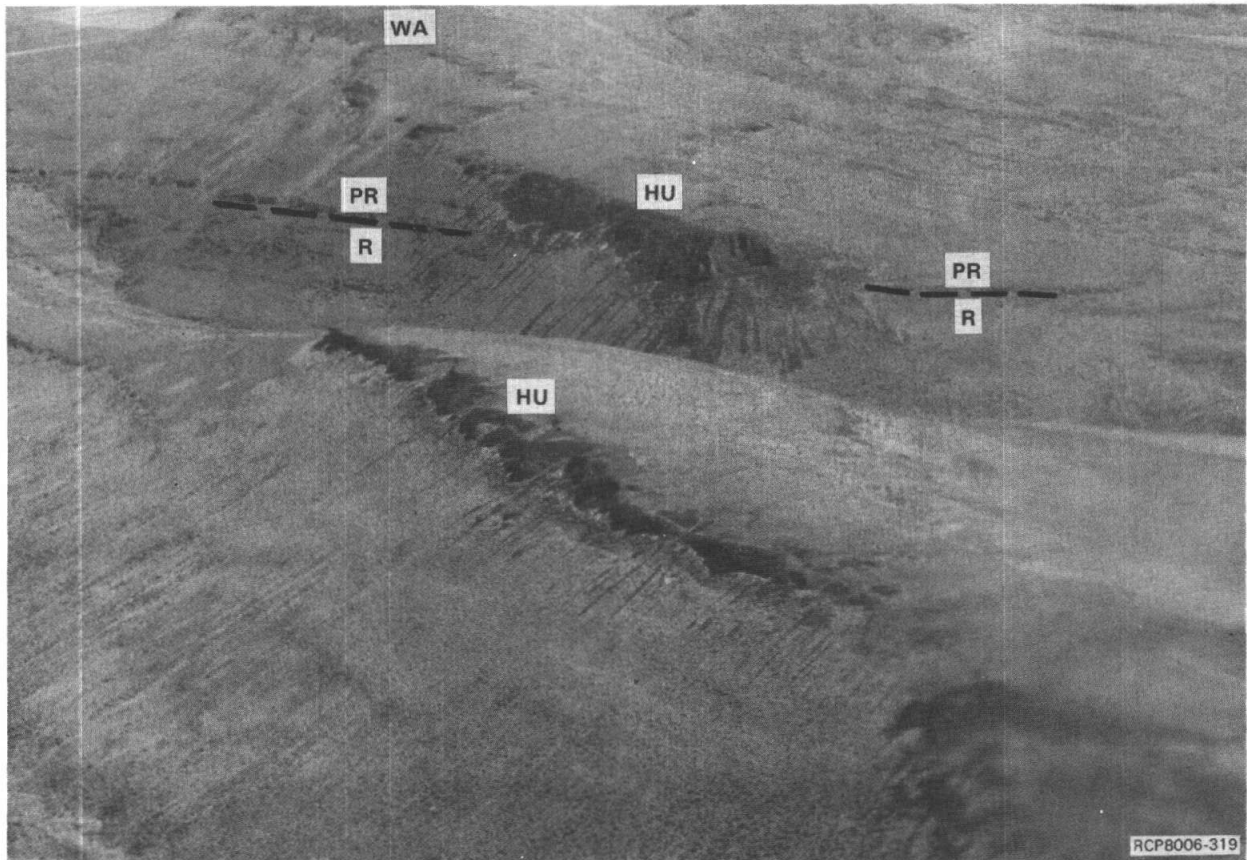


FIGURE 3. Huntzinger and Wahluke Intracanyon Flows. Huntzinger (Hu) and Wahluke (Wa) intracanyon basalt flows shown filling a paleocanyon cut in the Priest Rapids Member (Pr) and Roza (R) flow. The flow capping the ridge in the center foreground is Huntzinger; NE 1/4, Sec. 24, T13N, R323E; southwest of Emerson Nipple; view looking northeast.

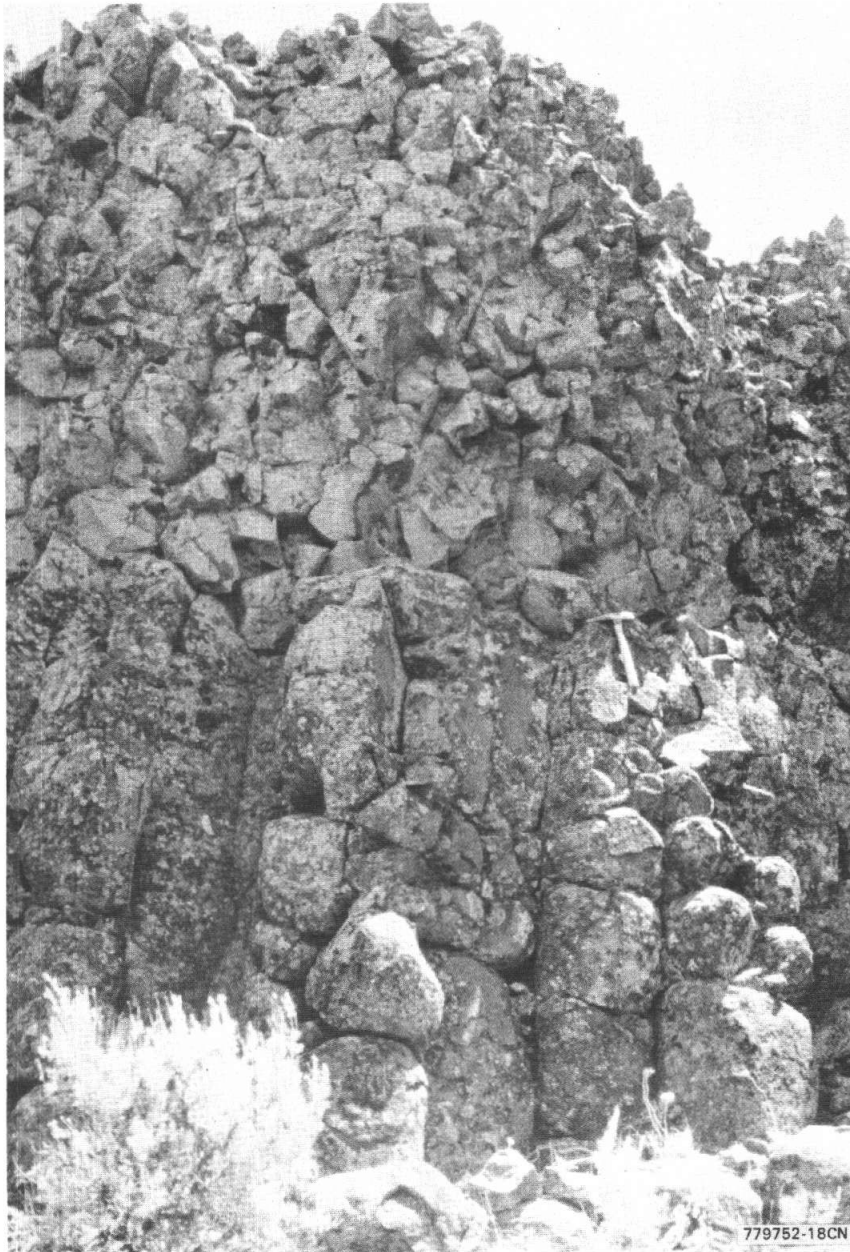


FIGURE 4. Colonnade and Entablature of Huntzinger Flow. Flow shown is that which caps the ridge in Figure 3.



FIGURE 5. Pillow-Palagonite Complex. Pillow-palagonite complex is exposed at the base of the Umatilla Member along Cold Creek. Exposure is nearly 30 meters thick. Foreset bedding in elongate pillows indicates that the basalt flowed toward the west and northwest; center Sec. 30, T13N, R24W. View looking north.

contain sparse phenocrysts, and so closely resemble the Umatilla that positive identification requires analysis of chemical composition.

The Umatilla is best exposed in the core of the Cold Creek syncline, where it forms a black cap on several north-south-trending ridges. Its chief characteristics are an aphyric, glassy texture and concoidal fracture. Primary flow features are poorly exposed, but the Umatilla generally forms rounded slopes covered with fist-sized pieces of the entablature. The base of the Umatilla in the Cold Creek syncline is a zone of pillows, locally greater than 25 meters thick, coated with yellow clay derived from palagonite (Figure 5). Thin, discontinuous outcrops of gravel, sand, silt, and chert from the Mabton interbed (Ellensburg Formation) underlie the Umatilla and help define the approximate base of the flow.

WANAPUM BASALT

Sheet-like flows of the Priest Rapids, Roza (or "Roza-like"), and Frenchman Springs Members comprise the Wanapum Basalt on eastern Umtanum Ridge.

The flows of the Priest Rapids Member are aphyric and generally diktytaxitic. Most outcrops have reverse, natural remanent magnetic polarity, but occasionally some outcrops, particularly in the uppermost flow, have normal polarity. In such cases, Priest Rapids flows can be distinguished from aphyric Frenchman Springs flows only on the basis of chemical composition. Lower flows of the Priest Rapids commonly contain abundant vesicle cylinders (Goff, 1976 and 1977). A prominent interbed of sand, silt, and chert fragments apparently underlies the uppermost flow of the Priest Rapids Member throughout most of the map area. This interbed may represent a major time interval between flows of the Priest Rapids and Lolo chemical types. Rare outcrops of siliceous silt of the Quincy (informal name) interbed appear as thin lenses at the base of the lowest Priest Rapids flow.

The Roza Member (Mackin, 1955) is very porphyritic and has transitional to reverse, natural remanent magnetic polarity. All porphyritic flows of the Wanapum Basalt on eastern Umtanum Ridge have

normal polarities except one (Table 3, Sample C2106), which is in the wrong stratigraphic position to be Roza. Therefore, the Roza Member on eastern Umtanum Ridge, based on field-determined, natural remanent magnetic polarities, may not be the Roza Member of Mackin (1955). Because of this lack of distinguishing chemical and field-determined physical characteristics between this member and the Frenchman Springs Member, this flow is referred to as the "Roza-like" member in this study. Chemical considerations are discussed in the section entitled Chemical Composition.

The Squaw Creek Member of the Ellensburg Formation, which separates the Roza and Frenchman Springs Members, is missing on eastern Umtanum and Yakima Ridges.

The Frenchman Springs Member consists of three mappable units which have normal, natural remanent magnetic polarities: (1) an upper porphyritic unit possibly equivalent(?) to the Roza Member and referred to by Reidel (1978) as the "Roza-like" unit; (2) a central aphyric unit; and (3) a basal porphyritic unit. Frenchman Springs flows were not subdivided in the northwest part of the map area. The porphyritic flows of the Frenchman Springs Member are key reference horizons for mapping the Wanapum Basalt because the glomeroporphyritic textures are easily recognized. Hand specimens of aphyric Frenchman Springs, however, are very difficult to distinguish from Priest Rapids or upper Grande Ronde samples. In addition, the primary flow characteristics and outcrop appearances of Wanapum lavas are similar to one another.

The Vantage Member of the Ellensburg Formation crops out as a discontinuous layer of mica-bearing feldspathic sandstone underlying the Frenchman Springs Member. The Vantage Member is the major stratigraphic marker on the upper portion of the north face of Umtanum Ridge, because no flows exposed below this horizon (Grande Ronde flows) are glomeroporphyritic. The Vantage horizon can be followed visually at a distance by the small topographic bench it generally forms and by the occurrence of many small, cold springs with their accompanying vegetation.

GRANDE RONDE BASALT

Basalt flows beneath the Vantage interbed (Ellensburg Formation) of the Grande Ronde Basalt are the most difficult to differentiate because all hand samples are generally black and aphyric, natural remanent magnetic polarities are normal, and whole-rock chemical compositions are very similar (see Figure 2 and Table 3). Grande Ronde Basalt crops out in the map area only on the north face of Umtanum Ridge. A key marker horizon within this upper Grande Ronde Basalt is delineated by an abrupt change in chemical composition, particularly magnesium oxide abundance, of the lavas on either side of the horizon (Ledgerwood, 1973; Myers, 1973). This horizon is informally known as the "MgO horizon" (see Figure 2). The horizon occurs on Umtanum Ridge between two very thick flows with thick flow-top breccias that do not appear in other flows. This breccia locally attains a thickness of 50 meters in the lower flow (informally termed the Umtanum flow). Recognition of the Umtanum flow is important because it, along with other thick flows, is one of the flows being considered as a host rock for repository construction beneath the Hanford Site.

In general, based on data gathered during this study, most Grande Ronde Basalt flows do not have distinctive physical traits that can be recognized in the field. Field traits were revealed during study of the McCoy Canyon stratigraphic section (Plate 2). These traits (see Table 2) may be useful for flow characterization during sample logging of flows penetrated during rotary and core drilling beneath the Hanford Site.

CONTINUITY OF INDIVIDUAL FLOWS

Columbia River basalt filled the Pasco Basin with layer after layer of lava flows that are, in some cases, traceable for many kilometers. However, not all flows, particularly the thinner ones, have this continuity. As an example, the flow with vesicle cylinders (Flow 8) in the McCoy Canyon stratigraphic section (Plate 2) is thinner and does not occupy the same stratigraphic position as the apparently equivalent flow exposed in another continuous basalt section 3 kilometers to the west.

This section can be observed in the deep canyon in the SE 1/4, Sec. 12, T13N, R23E. A sketch of the lower part of this section appears in Figure 6.

The chemistry of these two flows is nearly the same, with consideration of the limits of analytical methods used in this study (Table 3, Samples C2062 and C2133). The flow represented by sample C2061 (Figure 6) is apparently not present in the McCoy Canyon section (Plate 2). A possible explanation for these stratigraphic differences in such short distances would be a barrier, perhaps a fault or a flow margin, that blocked more widespread distribution of the flow (sampled by C2061). In addition, at least one Grande Ronde flow pinches out on Umtanum Ridge (NE 1/4, Sec. 17, T13N, R24E).

THE FLOW-TOP BRECCIA PROBLEM

The Umtanum flow and the flow above it display thick, flow-top breccias in the McCoy Canyon section (Plate 2). The flow-top breccias contain pieces of non-oxidized, vesicular basalt in nearly the same proportions as massive, non-vesicular basalt. The margins of the clasts are often glassy and the matrix between the clasts commonly appears to have been derived from palagonite. Within the breccia are lenses of intact massive basalt interpreted to have invaded the breccia as a liquid after the breccia was emplaced. Other flows throughout the Pasco Basin region locally contain zones of these breccias. The thickness and manner of occurrence of these breccias vary from place to place, both in outcrops and in subsurface drill holes. The origin of such breccias is not understood. They are unlike typical vent breccias which contain primarily oxidized scoria, spatterbombs, and rewelded lava. These breccias do not resemble tectonic breccias, because they do not normally contain discrete shear planes, slickensides, or mylonitic matrix, nor are they related to any offset in layering. They are, therefore, interpreted in this report as primary flow features. Should future work indicate the breccias to be vent related, the presence of such breccias may indicate nearby, previously unrecognized vents.

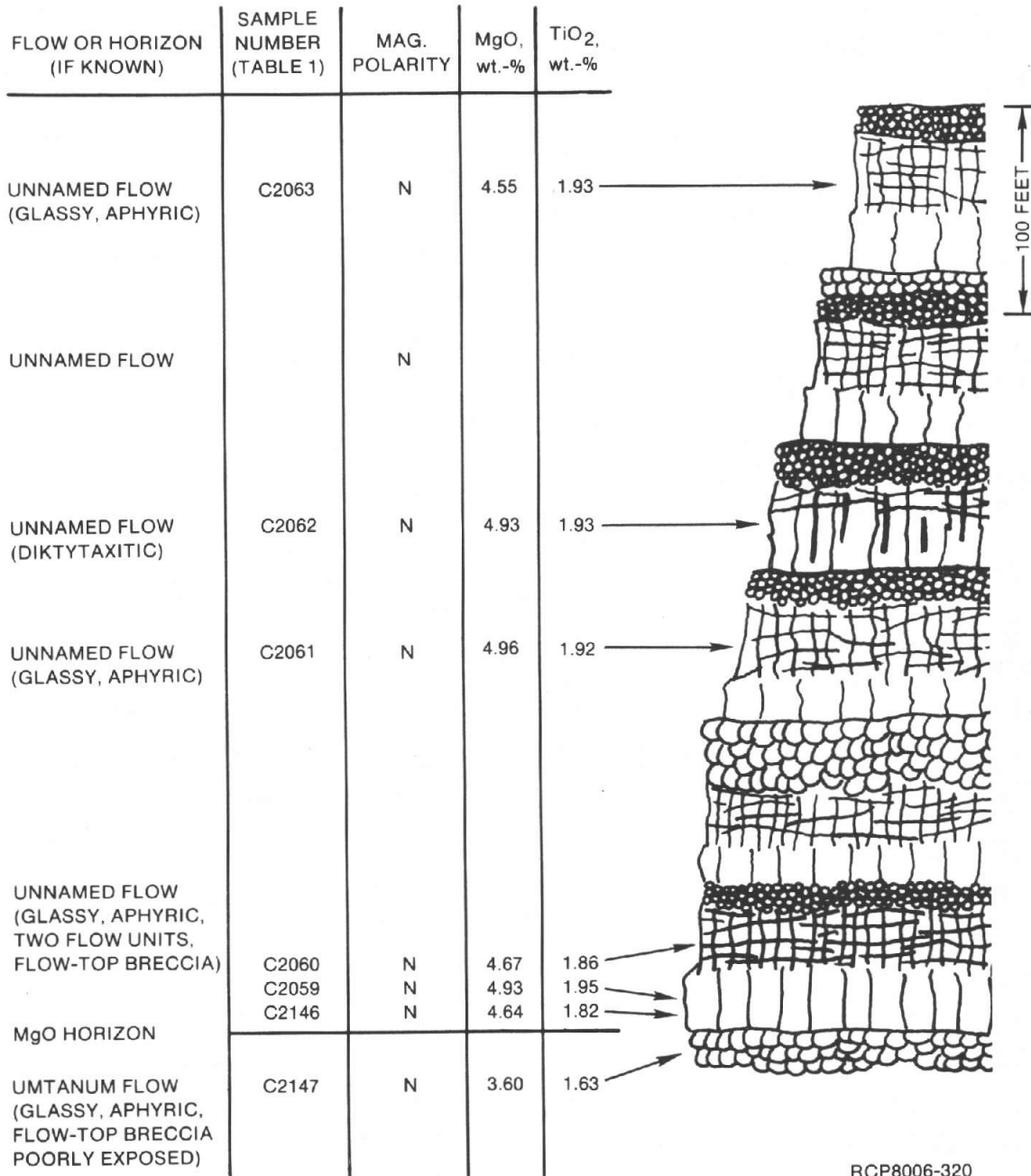


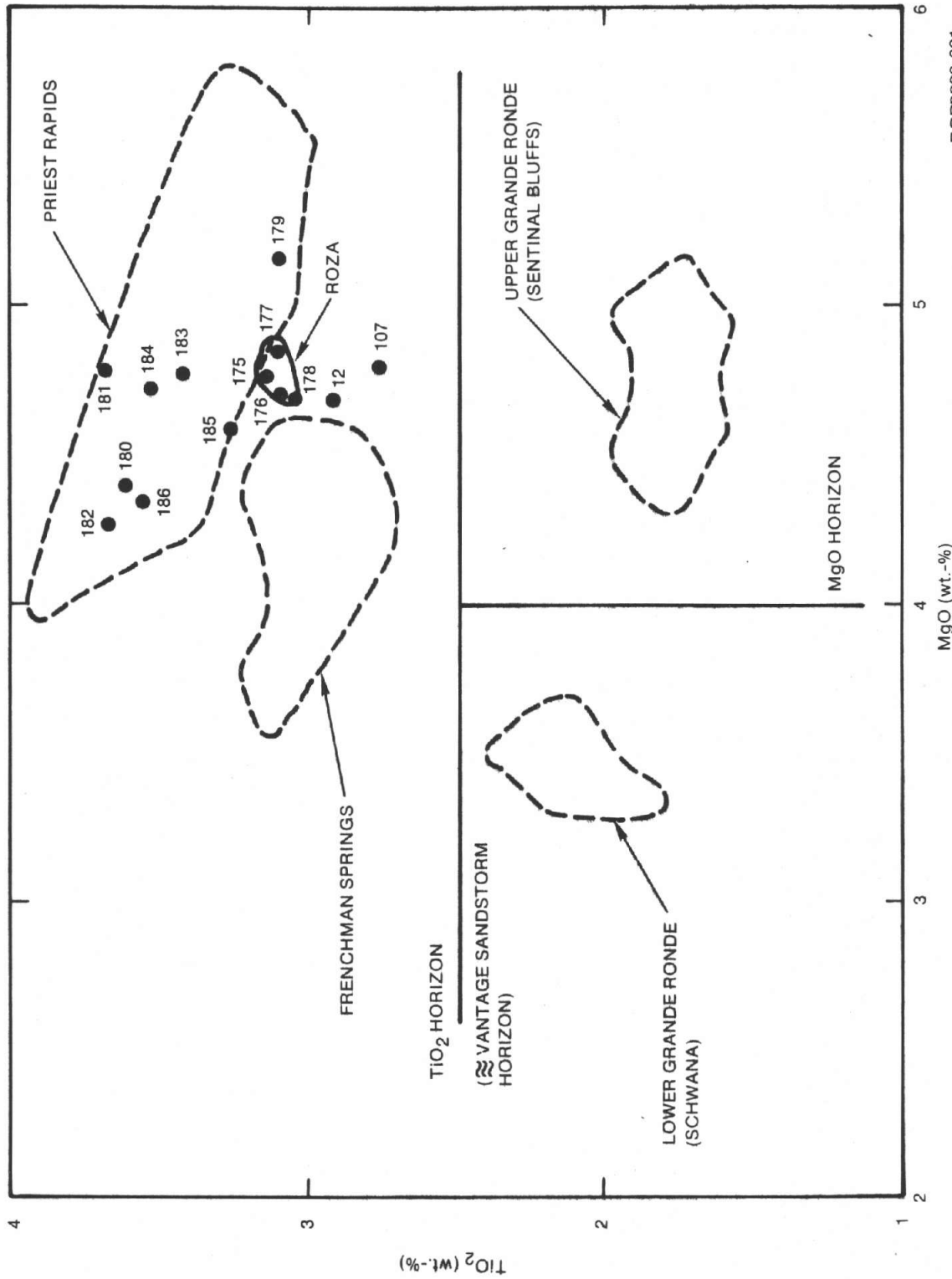
FIGURE 6. Partial Columnar Stratigraphic Section. Section is in the SE 1/4, Sec. 12, T13N, R23E. Scale approximate. See Plate 2 for explanation of symbols.

The Umtanum flow and the overlying flow are also glassy and aphyric, with a concoidal fracture; yet these flows are generally over 60 meters thick throughout much of the Pasco Basin. The thickness and distribution of these flows suggest they were once lava lakes formed by ponding in an ancestral Pasco Basin. Thick flows forming lava lakes would, under some circumstances, remain partially molten for tens to hundreds of years and develop partially crystalline to porphyritic textures (Moore and Evans, 1967). However, the Umtanum flow and the flow above are distinctly aphyric.

These glassy flows and thick flow-top breccias may have a common genetic affinity. The following hypothesis for their origin was offered by Dr. A. C. Waters in 1979. Large rivers such as the Columbia and the Snake were flowing through a paleobasin (not necessarily the present Pasco Basin) during Umtanum time. As the Umtanum flow was emplaced and ponded, it displaced and locally dammed the flow of the large rivers. The displaced water is interpreted to have flooded over the surface of the evolving lava lake. Instead of forming pillows, such as when lava pours into a body of water, the water flowing over the top of the flow quenched the surface of a lava lake. The rapid chilling, the large volume of water flashing to steam, and the foundering of unstable flow crust would churn the upper one third to one half of the flow into the chaotic breccias seen in outcrop. This thick layer of relatively cold, water-soaked breccia would overlie the remaining liquid layer of lava from the lava lake. Normal cooling would continue in this underlying lava layer, but would result in formation of a thinner entablature and colonnade than would be found in an undisturbed, air-cooled lava lake of equivalent thickness.

CHEMICAL COMPOSITION

Approximately 100 basalt samples were chemically analyzed for use in identification and correlation of basalt units (Table 3). Variation diagrams of key oxides and elements were constructed (Figures 7 and 8) from these data and compared with type locality analyses obtained from Brock and Grolier (1973), ARH-ST-137 (1976), and X-ray fluorescence analyses supplied by Washington State University under contract to



RCP8006-321

FIGURE 7. Variation of MgO Compared to TiO_2 - Priest Rapids, Frenchman Springs, Grande Ronde Basalt. Diagram shows chemical variation fields for Priest Rapids, Frenchman Springs, and Grande Ronde Basalts. See text for discussion of numbered points. Except for the Roza field, which is plotted using X-ray fluorescence data, all field boundaries are drawn from data presented in Table 3.

Rockwell during 1977. Although many plots are useful, only one (the plot of variations of MgO compared to TiO_2) is necessary to distinguish most of the different basalt members on Umtanum Ridge. Wright and Others (1973) give an in-depth discussion of chemical stratigraphic variations in Columbia River basalt.

The Priest Rapids, Frenchman Springs, and Roza Members and the Grande Ronde Basalt are distinguishable on the basis of unique groupings on the MgO- TiO_2 variation diagram (Figure 7). Some uncertainty exists regarding the validity of placement of the Priest Rapids-Frenchman Springs fields if only a few analyses are used to construct such a variation diagram. However, the dashed fields outline 21 Priest Rapids analyses and 24 Frenchman Springs analyses from Table 3. Although the fields are diffuse and close to one another, they are distinct. Points numbered 179-186 are X-ray fluorescence analyses of samples from the Priest Rapids Member taken from core hole PRK-3 which was drilled during construction of Priest Rapids Dam (Mackin, 1955). Also shown in Figure 7 is the field defined by four X-ray fluorescence analyses (Numbers 175-178) of samples from the Roza Member in Frenchman Springs Coulee (Mackin, 1961). The Roza Member data plot as a field separate from the Priest Rapids and Frenchman Springs fields, although Drs. D. A. Swanson and T. L. Wright of the U.S. Geological Survey consider the Roza to be chemically indistinguishable from the Frenchman Springs based on more extensive sampling and chemical analyses. The apparent difference in chemical composition is consistent with a parallel difference in natural remanent magnetic polarity data, indicating that this may be an upper Frenchman Springs flow and not the Roza. However, the difference in chemical composition may be more apparent than real. This apparent distinction is worthy of further, more detailed study; but for the purposes of the present geologic mapping, the upper porphyritic Frenchman Springs unit has been identified as the "Roza like" member.

Analyses 12 and 107 on Figure 7 (Samples C2012 and C2107, Table 3) are from Priest Rapids samples that are outside of the Priest Rapids variance field. Sample C2107 contains nearly 5% water which, if not adjusted for, lowers the true value of MgO and TiO_2 . The anomalous position of Sample C2012 on the variation plot is not understood.

In contrast to the vague separation between the Frenchman Springs and Priest Rapids data variance fields (Figure 7), the separation between Wanapum and Grande Ronde chemical variance fields (TiO_2 horizon) and the upper (Sentinel Bluffs) and lower (Schwana) Grande Ronde units (MgO horizon) is very distinct. Chemical composition data are essential to map the MgO horizon across the folded and somewhat poorly exposed ridges west of Priest Rapids Dam. The TiO_2 horizon is in appropriate stratigraphic position to coincide with the Vantage Member on Umtanum Ridge.

The usefulness of TiO_2 variance compared to MgO variance is shown again in Figure 8, which clearly identifies the majority of members in the Saddle Mountains Basalt. The variance fields were defined by plotting data from ARH-ST-137 (1976) with additional Umatilla and Pomona analyses from Brock and Grolier (1973). Numbered points representing atomic absorption data are presented in Table 3, except for Number 194 of the Wahluke flow (X-ray fluorescence data, Washington State University). If the additional atomic absorption and X-ray fluorescence data can be considered statistically significant, then the range in composition of the Umatilla and Wahluke flows is larger than that suggested by the earlier data. (The Wahluke chemical variance field was drawn from only two analyses.) Ambiguity exists only in separating the Huntzinger (Samples C2067, C2094, and C2140, Table 3) from the Pomona (Samples C2004, C2050, C2071, C2072, C2112, and C2143, Table 3) flows. Analysis Number 72 on Figure 8 is from a sample of weathered flow bottom of the Pomona which plots anomalously due to its relatively high water content (5%). The Huntzinger and Pomona flows can be distinguished at the outcrop on the basis of magnetic polarity as noted above. Potassium oxide concentration can be used to distinguish the Huntzinger flow (>1%) from the Pomona flow (<11%).

Barium concentration can be used to identify the Umatilla flow (>2,500 parts per million (ppm)) and Wahluke flow (approximately 1,100 ppm) from other members of the Columbia River Basalt Group (<1,000 ppm).

A diagram showing CaO-MgO variance is especially useful for separating the Elephant Mountain Member from Wanapum basalts if field criteria do not suffice. However, no Elephant Mountain Member appears on

eastern Umtanum Ridge, and only one Elephant Mountain sample (Number 77) comes from Yakima Ridge.

The key constituents for identification of Columbia River Basalt members are thus MgO, TiO₂, CaO, and Ba. K₂O may be useful for distinguishing the Huntzinger and Pomona flows. FeO and MnO do not appear to vary enough between different members to be useful stratigraphic markers. The atomic absorption analyses of SiO₂, Al₂O₃, and P₂O₅ listed in Table 3 are considered to be unreliable for identification of basalt units based on comparison with analyzed standards and should be used with caution.

STRUCTURE

INTRODUCTION

Three major structures occur on eastern Umtanum Ridge: (1) an asymmetric west- to northwest-trending anticline; (2) a reverse fault with associated shear zones located along the tightly folded north limb of the anticline; and (3) a northwest-trending zone of deformation coinciding with the Olympic-Wallowa Lineament. The anticline and reverse fault are interpreted to be closely related in time and space; the latter being the final stage of development of the former. Folding has also taken place on Yakima Ridge, located to the south, and is similar but less pronounced than the folding events recorded on Umtanum Ridge. Minor structures on Umtanum Ridge include scattered normal faults with limited extent and minor displacement.

UMTANUM ANTICLINE

The Umtanum anticline is essentially a broad parallel fold (Class 1B of Ramsay, 1967) in brittle layers of Columbia River basalt, but the basic geometry has been modified by major reverse faulting along the north limb of the fold. The cliffs of the north face of the ridge expose mappable anticlinal and monoclinical fold hinges which are locally ill defined and which lie south of a belt of nearly vertical to overturned

basalt strata. Associated with these structures are several shear zones that are subparallel to the fold hinges and that are concentrated in areas of tightest folding.

Because the basalt flows have remained near the surface of the earth since their eruption, they have been folded under conditions of low temperature and low-confining pressure, and have thus behaved as brittle, rather than ductile, strata. In the gently folded regions, the primary flow features (i.e., cooling joints, vesicular flow tops) are perfectly preserved with no superimposed fracturing or foliation due to tectonism. The thickness of each basalt flow has remained uniform throughout the stages of folding, except along the monoclinial axis and shear zones.

Folding near the monoclinial axis (Figure 9) has apparently followed a flexural slip mechanism (Ramsay, 1967) with slip localized along the boundaries between basalt strata. Flexural slip is indicated by slickensides, scuffing, and grooving preserved in the upper surfaces of the less-competent flow tops and flow-top breccias of the basalts (Figures 10 and 11). Near areas of tight folding, horizons of flow-top breccia occasionally appear to have undulatory thicknesses (and boundaries), perhaps suggesting relative ductility compared to the more competent entablature and colonnade. Locally, the folding is so tight that shear zones have developed in the closure (Figure 12), the continuity of stratification is lost, and the dips of basalt layers are chaotic due to rupture from probable small-scale faulting (Figure 13).

Deformation of the colonnade and entablature has produced highly fractured outcrops which are cut by shears (Figure 14). Shear zones expressed by fractured, brecciated, and mylonitized basalt anastomose with one another subparallel to the fold hinge and are concentrated near the regions of tightest folding; some areas of sheared rock are isolated, however. The shear zones pinch and swell in thickness and their intensity of shearing varies; thus, their boundaries are only approximately located on the geologic map (Plate 1).

Major tectonic fractures appear to have three sets of preferred orientation: (1) a set striking sub-parallel to the fold hinges; (2) a conjugate fracture set striking sub-orthogonally to the fold hinges

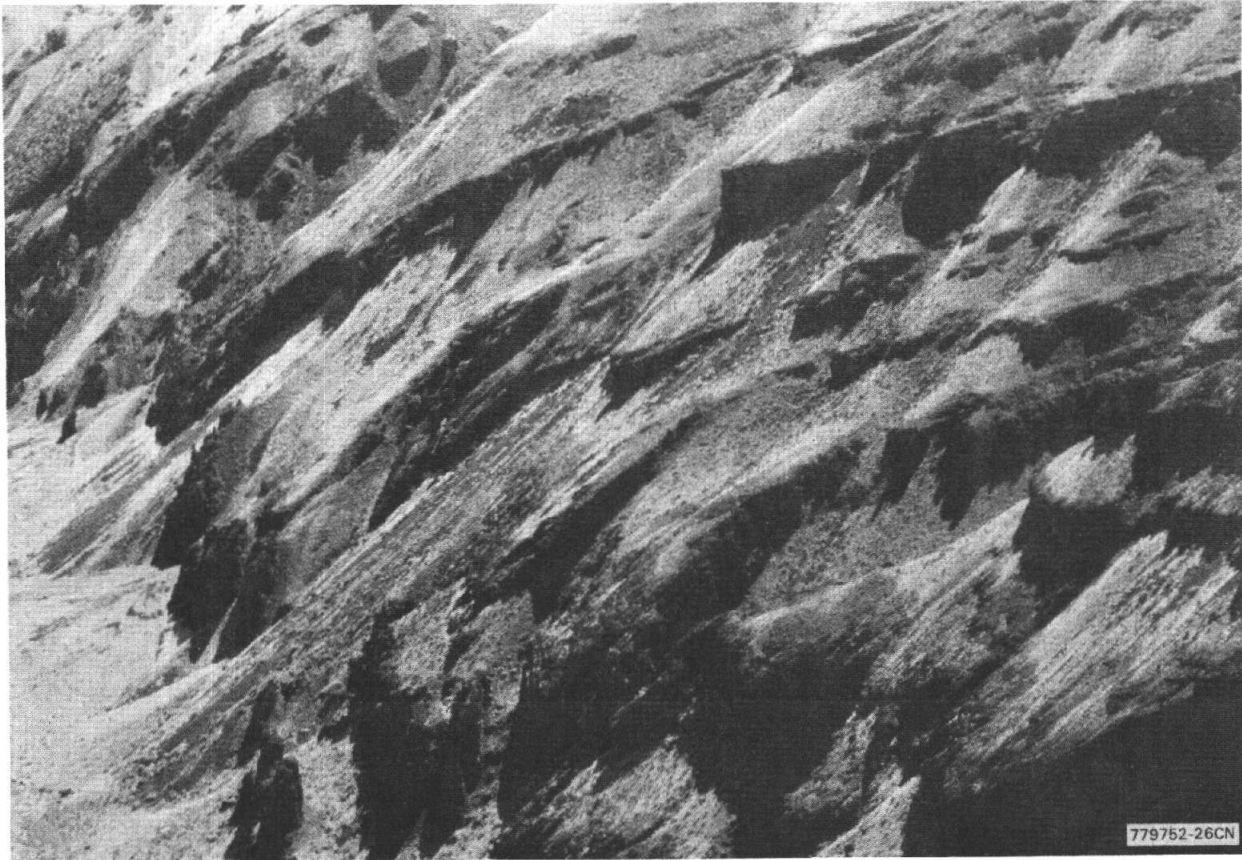


FIGURE 9. Tightly Folded Monocline--North Limb of Umtanum Anticline.
Sec. 16, T13N, R24E. View looking east.



FIGURE 10. Pitted and Grooved Flow Top in Monocline. North face of eastern Umtanum Ridge. The grooving is most pronounced at the fold hinge of this basalt flow. Flow appearance suggests flexural slip may have been the folding mechanism. Sec. 16, T13N, R24E. View looking south.

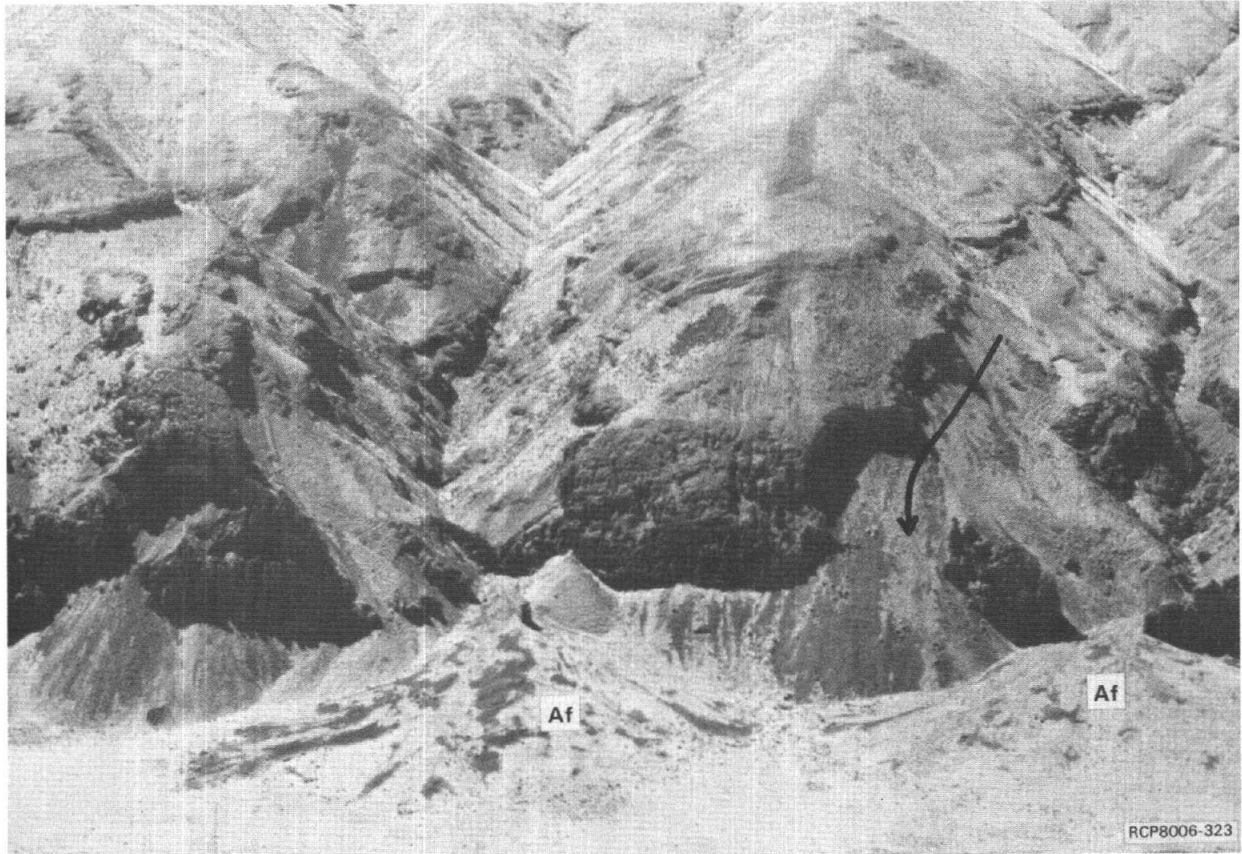


FIGURE 11. Umtanum Ridge Monocline. View of the Umtanum Ridge monocline east of the McCoy Canyon slide complex. Prominently exposed basalt layer is tightly folded at the nose of the ridge (arrow is perpendicular to the fold axis). The folding shown is associated with considerable tectonic fracturing. Alluvial fans (AF) fill canyon mouths. Note grooving on fold front. S 1/2, Sec. 8, T13N, R24E. View looking south.

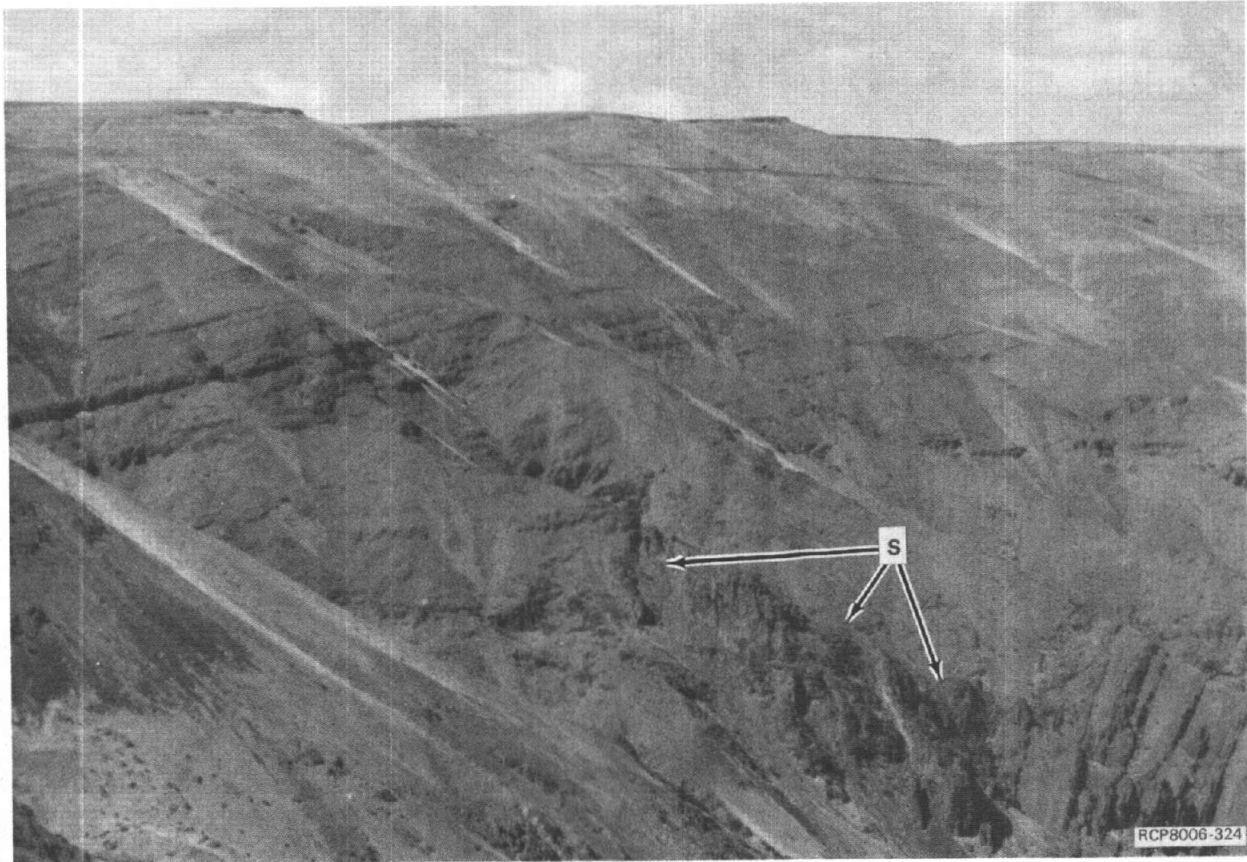


FIGURE 12. Shear Zone. Shear zone(s) is in the nose of the fold between nearly horizontal basalt strata (left side of photo) and vertical basalt strata (right side of photo). Porphyritic Frenchman Springs basalt caps ridge. View to west. West edge of Sec. 11, T13N, R23E.



FIGURE 13. Close-up View of Shear Zone. Close-up view of the shear zone shown in Figure 12 shows discordant dips (D) of basalt units at the south (left) margin of the shear zone. Folding in this zone has caused local, small-scale, reverse faulting.



FIGURE 14. Fractured Entablature Zone in a Flow of Grande Ronde Basalt. Note the two vertical shear planes(s). Shear plane on right is slickensided (Sample C2058, Table 4).

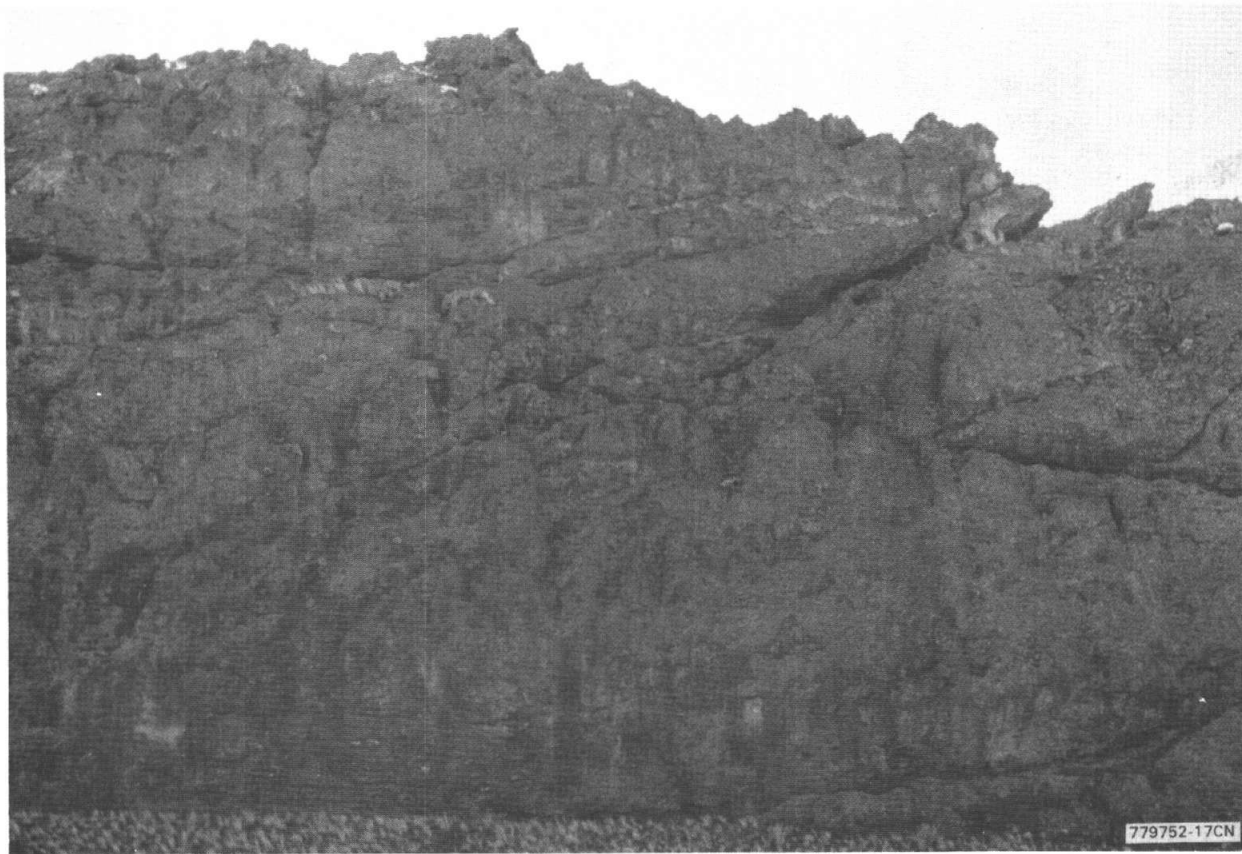


FIGURE 15. Criss-crossing, Tectonically Induced Fractures. Fractures are in vertically standing basalt layer. View looking south is of an east-west-striking flow of Grande Ronde Basalt. N 1/2, Sec. 15, T13N, R24E.

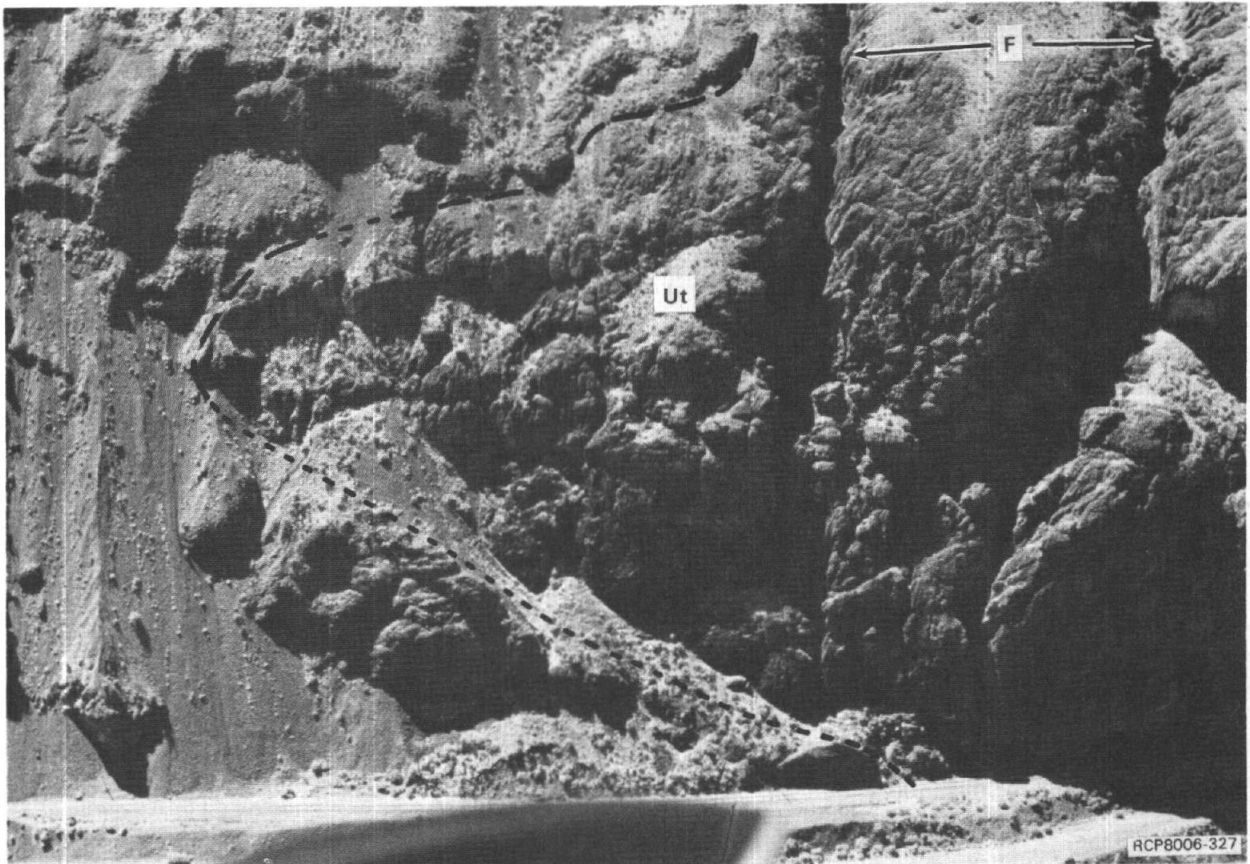


FIGURE 16. Intensely Folded and Fractured Umtanum Basalt Flow. The photo shows tectonic deformation of the Umtanum (Ut) and an overlying flow in the Umtanum monocline east of the McCoy Canyon slide complex. The contact between the two flows (MgO horizon) is shown as a dashed and dotted line. Two very prominent fractures (f) trend perpendicular to the the fold axis, as do many other, more subdued fractures. SE 1/4, Sec. 8, T13N, R24E. View is due south.

(Figure 15); and (3) a set orthogonal to the fold hinges (Figure 16). Fractures of the first set are generally orthogonal to the stratification between flows. Fracture planes of the second set are nearly horizontal in vertically standing basalt strata (Figure 15). In such outcrops, the fractures criss-cross in conjugate patterns with interior angles of roughly 60 degrees.

Tectonic fractures and shear zones cut through many layers of basalt strata on eastern Umtanum Ridge; they are not confined to single layers. These structures are thus present (but less distinct) in the flow-top breccias which were already fragmented by primary processes prior to tectonic fracturing.

PHYSICAL CHARACTER OF SHEARED BASALT

Samples of sheared basalt from the colonnade or entablature units consist of lenticular fragments of basalt in a dark grey to brown, fine-grained groundmass (Figures 17 through 24). The major shears generally have one preferred orientation, criss-crossed by discontinuous fractures of random orientation. Some samples display two preferred orientations of shear which give rise to phyllitic or schistose textures. Many of these samples are slickensided. Still other samples contain sparse fragments of basalt in a fine-grained matrix with no obvious preferred orientation (Figure 20).

Study of these sheared samples in thin section reveals that the matrix between the lenticular fragments is predominately pulverized basalt (Table 4). Shearing has milled down the basalt pieces into a mixture of submicroscopic rock flour and basalt micro-breccia which occasionally displays a banded texture. The submicroscopic rock flour surrounding the fragmented basalt was examined by X-ray diffraction analysis and found to be predominantly mylonitized basalt (Table 5). No recrystallized (metamorphic) textures were observed.

Secondary minerals filling fractures include mostly erionite (high-K zeolite, Table 6), calcite, and Fe oxides. Little or no argillization is present. The erionite commonly displays undulatory extinction under crossed-polarized light.

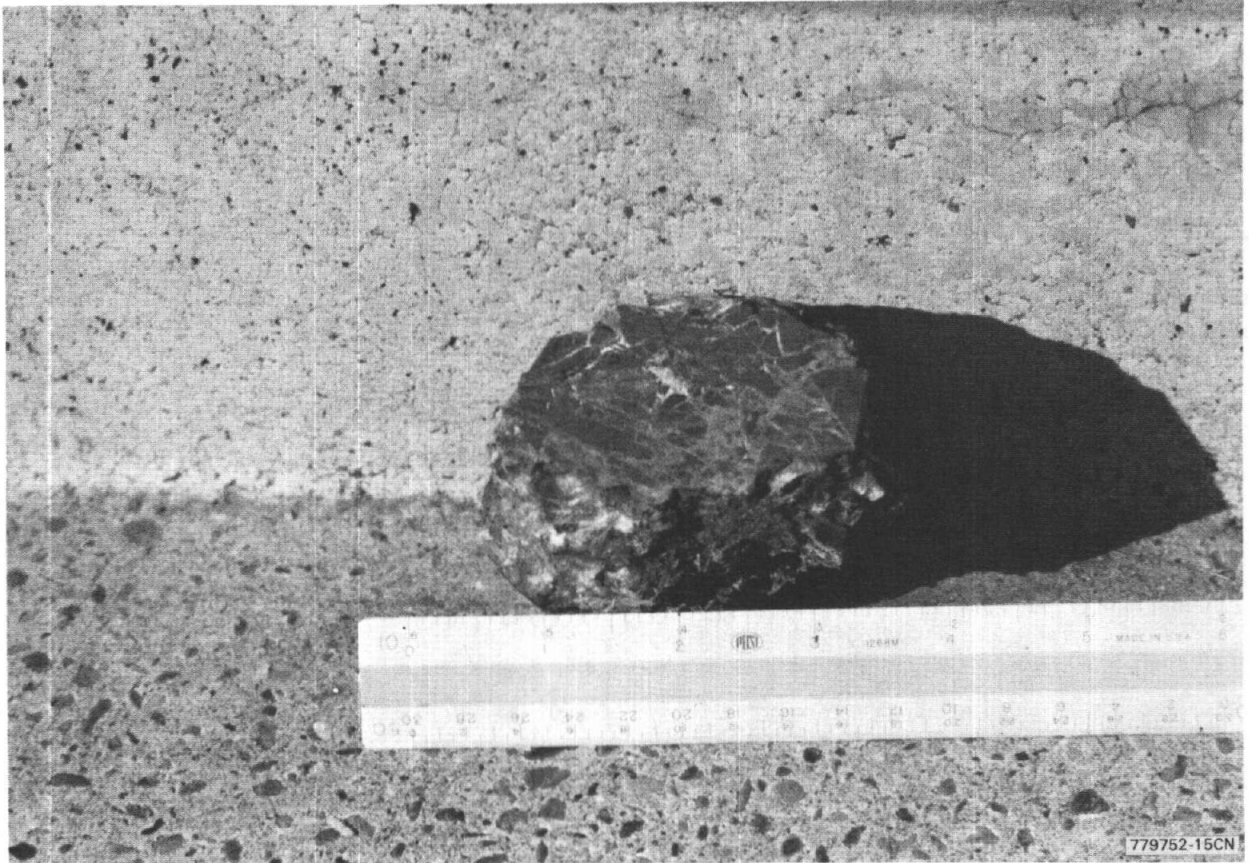


FIGURE 17. Sawed Surface of Fractured and Sheared Aphyric Basalt. The sample shown (C2001B, Table 4) is from a shear zone in the Grande Ronde Basalt, Sec. 15, T13N, R24E.



FIGURE 18. Photomicrograph of Sample 2025B (Table 4). Sample is of sheared basalt; open fractures are filled with erionite and fragments of basalt. Plane polarized light. Magnified 65x.



FIGURE 19. Photomicrograph of Sheared Basalt, Sample 2025B (Table 4). Shown are fractured pyroxene (P) and erionite (e); undulatory extinction). Crossed polarized light. Magnified 65x.



FIGURE 20. Extensively Brecciated and Mylonitized Aphyric Basalt, Sample C2025C (Table 4). White splotches visible in the photograph are mostly carbonate. Magnified 65x.



FIGURE 21. Photomicrograph of Sheared Basalt, Sample 2025C (Table 4). The open fracture in the center of the field of view has been sealed with carbonate which engulfs fragments of basalt. Crossed polarized light. Magnified 65x.



FIGURE 22. Photomicrograph of Sheared Basalt, Sample C2046 (Table 4). Fractures are filled with pulverized basalt. Crossed polarized light. Magnified 65x.

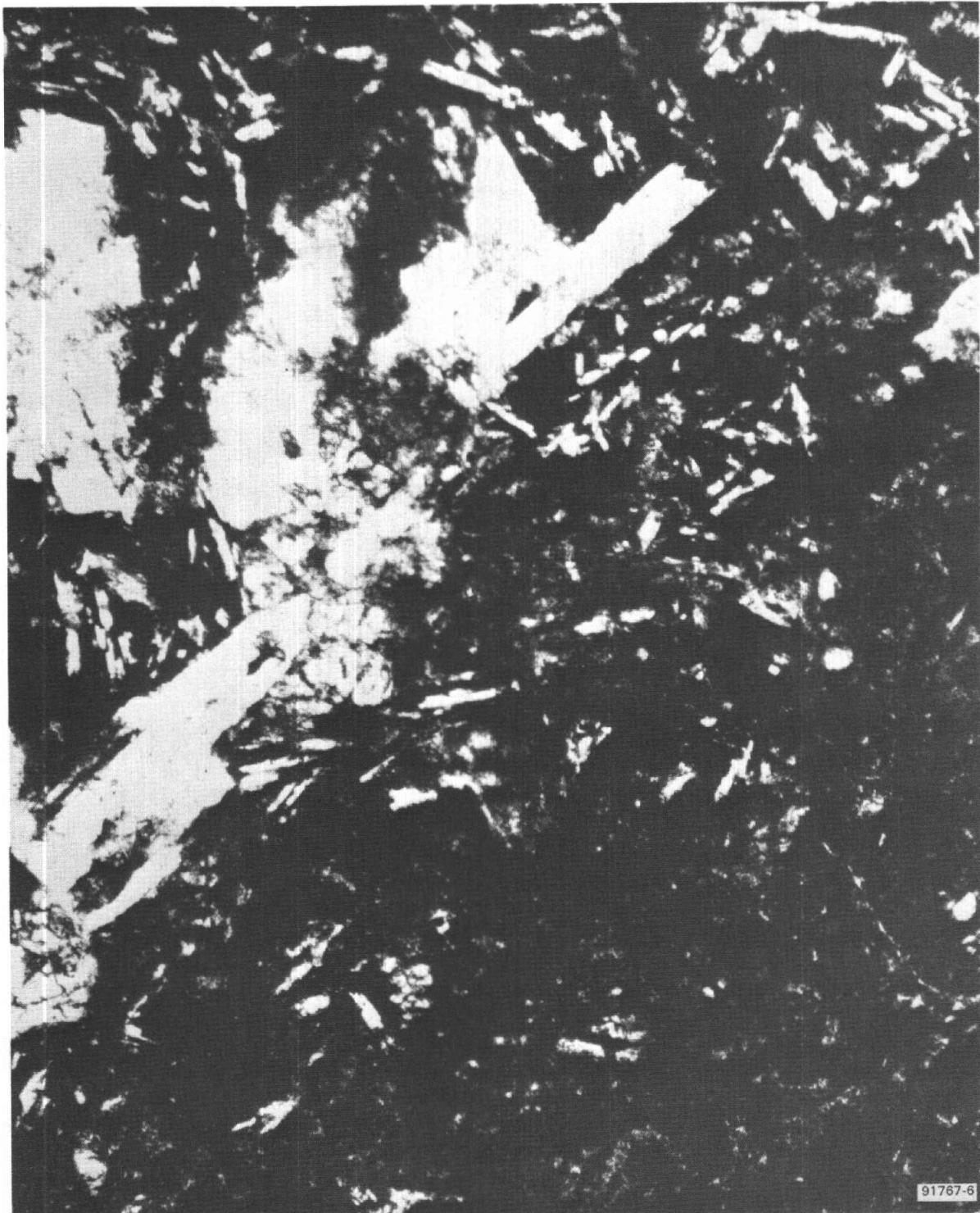


FIGURE 23. Photomicrograph of Sheared Basalt, Sample C2058 (Table 4). Shown are mylonitized zone of pulverized basalt (dark area in lower right corner of field of view) and crushed plagioclase phenocrysts (p). Plane polarized light. Magnified 65x.

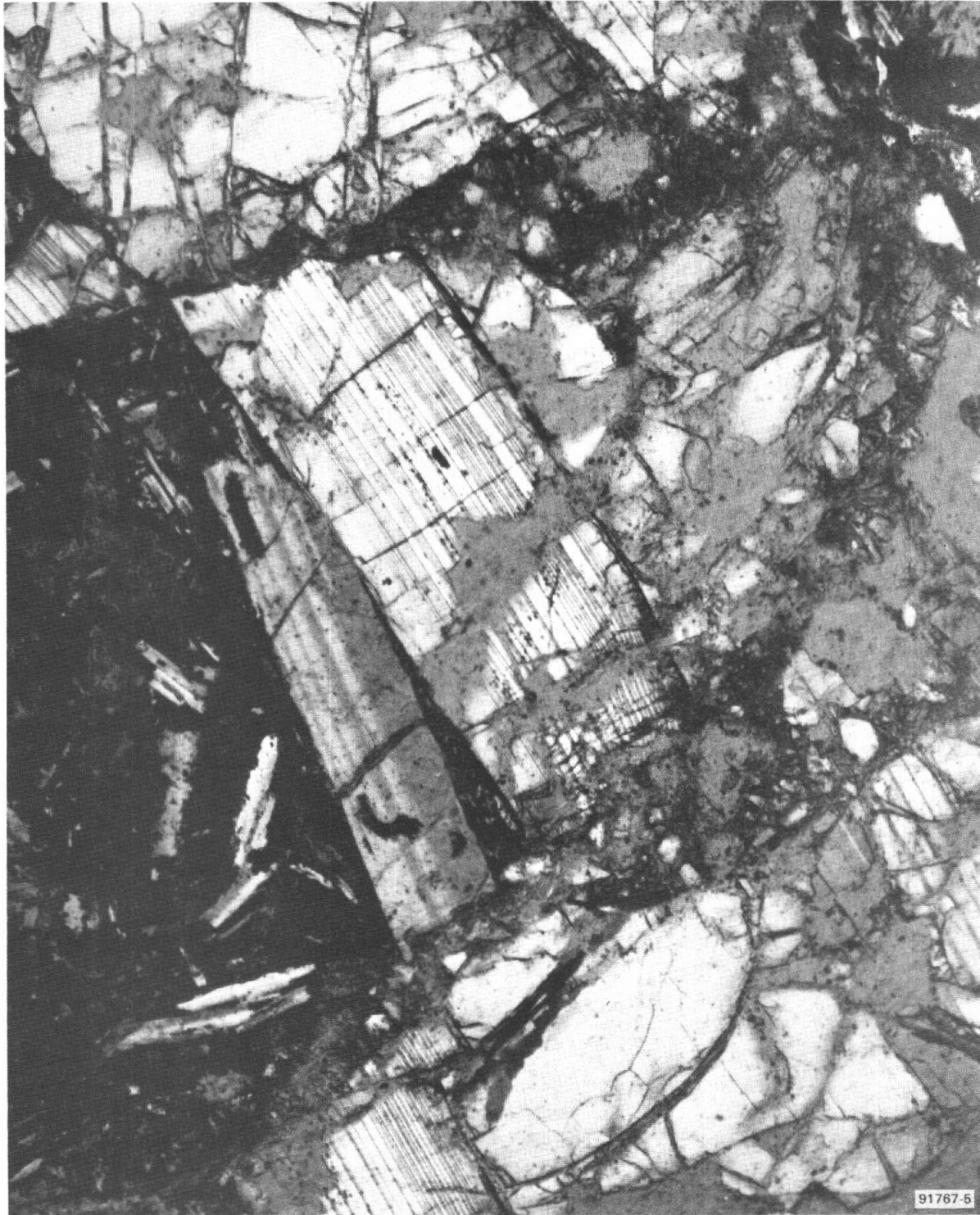


FIGURE 24. Photomicrograph of sheared plagioclase phenocryst, Sample C2069 (Table 4). Note offsets in albite-twinned plagioclase. Approximately 550-meter wave length retardation. Crossed polarized light. Magnification 65x.

TABLE 4. Descriptions of Tectonically Deformed Basalts from Eastern Umtanum Ridge.

Sample	Member	Location	Description
C2001B	Tsb (Rocky Coulee Basalt?)	Sec. 15, T13N, R24E	Highly fractured and sheared aphyric basalt with moderate directional orientation of angular fragments; displacement along individual fractures is probably minor, as measured by offset of plagioclase microphenocrysts; matrix between fragments consists mainly of pulverized basalt with minor Fe oxides, carbonate, and clay(?).
C2025B	Tsu (Umtanum Basalt)	Sec. 17, T13N, R24E	Highly sheared aphyric basalt with two planar cleavages that give the specimen a phyllitic appearance; only minor displacement observed between angular fragments as measured by offset of microphenocrysts; matrix between fragments is erionite (high-K zeolite), pulverized basalt, minor Fe oxides, carbonate, and clay(?); the erionite does not have uniform optical extinction, suggesting deformation of the basalt contemporaneous to formation of the mineral.
C2025C	Tsb	Sec. 7, T13N, R24E	Brecciated and mylonitized aphyric basalt; scattered basalt fragments are laced with fractures filled with carbonate; mylonitized zones consist of rounded basalt blebs surrounded by a submicroscopic paste of plagioclase, pyroxene, and glass (X-ray diffraction analysis); fractured zones resemble Samples C2001B and C2025B; offset in mylonitized zones is unknown.
C2046	Tfup	Sec. 19, T13N, R24E	Highly sheared and fractured porphyritic basalt with strongly directional orientation; angular fragments; appearance resembles Sample C2001B; matrix between fragments consists of pulverized basalt; offset along fractures is minor as suggested by offset of microphenocrysts.
C2056	Tsb (Museum Basalt)	Sec. 13, T13N, R23E	Crushed aphyric basalt with mixed patches of intact basalt; no directional orientation of fractures; many shattered and offset microphenocrysts; matrix between intact zones consists of pulverized and sheared basalt.

Table 4 (continued)

Sample	Member	Location	Description
C2058	Tsb	Sec. 12, T13N, R23E	Highly fractured and sheared basalt with distinct schist-like foliation; specimen resembles Sample C2025B; mylonitized zones consist of tiny basalt fragments in a submicroscopic paste of plagioclase pyroxene and glass (X-ray diffraction analysis); rare phenocrysts are shattered; some fractures contain erionite.
C2066	Tsu (Umtanum Basalt)	Sec. 12, T13N, R23E	Well-indurated flow-top breccia composed of glassy, vesicular, basalt clasts in a matrix of vesicular basalt; a definite shear fabric penetrates the primary texture, shattering large fragments and some phenocrysts; matrix along fractures appears to be primarily pulverized basalt.
C2067A	Tsu (Umtanum Basalt)	Sec. 12, T13N, R23E	Well-indurated flow-top breccia that resembles Sample C2066; shear fabric is less obvious, but pervasive.
C2069	Tfup	Sec. 13, T13N, R23E	Sheared and mylonitized flow-top breccia with slickensided shear zone; pervasive shears offset glassy basalt clasts, phenocrysts, and vesicular basalt matrix; slickensided zone consists of tiny basalt blebs in a submicroscopic matrix of plagioclase, pyroxene, and glass (X-ray diffraction analysis).

TABLE 5. Summary of X-Ray Diffraction Powder Data
 Submicroscopically Mylonitized Basalt Samples
 C2025C, C2058, and C2069 (See Table 4)*

d, A	Intensity	Peak Characteristic	Minerals**
6.23	w	Sharp	Plagioclase?
4.98	w	Sharp	?
4.48	s	Sharp	Clinopyroxene
4.04	s	Sharp	Plagioclase
3.75	s	Sharp	Plagioclase
3.35	w	Sharp	Clinopyroxene, Plagioclase
3.25	vs	Sharp	Plagioclase, Clinopyroxene
2.99	s	Sharp	Clinopyroxene, Plagioclase
2.94	s	Sharp	Clinopyroxene, Plagioclase
2.90	w	Sharp	Clinopyroxene
2.53	w	Broad	Plagioclase, Clinopyroxene
2.51	w	Broad	Plagioclase, Clinopyroxene
2.15	w	Sharp	Clinopyroxene
2.13	w	Broad	Plagioclase, Clinopyroxene
2.11	w	Broad	Plagioclase, Clinopyroxene

*40 KV, 1 ma, Ni-filtered Cu K α radiation, scanning speed =
 2 degrees 2 θ /min.

**ASTM index cards as follows: diopside, 11-654; andesine, 10-359;
 labradorite, 9-465. A broad rise in background from 16 degrees to 32
 degrees 2 θ is attributed to amorphous volcanic glass.

TABLE 6. Summary of X-Ray Diffraction Powder Pattern
of Erionite Fibers from Sheared Basalt,
Sample C2025B (See Table 4)*

d, A	Intensity	Peak Characteristic	Minerals**
17.6	w	Sharp	?
13.2	w	Sharp	?
11.78	vs	Broad	Erionite
9.82	w	Sharp	?
9.02	w	Broad	Erionite
8.11	w	Broad	?
7.37	w	Sharp	Erionite ?
6.75	s	Broad	Erionite
6.32	w	Sharp	Erionite
5.98	w	Broad	?
5.86	w	Broad	Erionite?
5.35	w	Broad	Erionite
4.59	w	Broad	Erionite
4.37	s	Sharp	Erionite
4.18	s	Sharp	Erionite
3.86	s	Sharp	Calcite
3.77	s	Broad	Erionite
3.60	s	Broad	Erionite
3.23	s	Broad	Erionite?
3.03	s	Sharp	Calcite
2.82-2.86	s	Broad	Erionite
2.57	w	Sharp	?
2.50	w	Sharp	Calcite,
Erionite			

*40 KV, 17ma, Ni-filtered Cu K α radiation, scanning speed =
2 degrees 2 θ /min.

**ASTM index cards as follows: calcite, 5-586; erionite, 12-275;
erionite, 22-854.

Deformation of flow-top breccias is more subtle in appearance than in other intraflow zones because the rock was already fragmented before tectonic shearing. However, a careful thin section study of the basalt clasts and their enclosing matrix reveals that the clasts have been sheared and that larger phenocrysts have been shattered (Figure 24). The amount of movement along the micro-shears in all types of samples is usually measureable in millimeters or less, judging from the offset displacement of microphenocrysts.

These "cataclastic" rocks are best categorized as protomylonites, cataclastites, and micro-breccias, using the definitions of Higgins (1971), and they resemble the cataclastic rocks found in the fault plane of the Wallula Gap fault (Gardner, 1977).

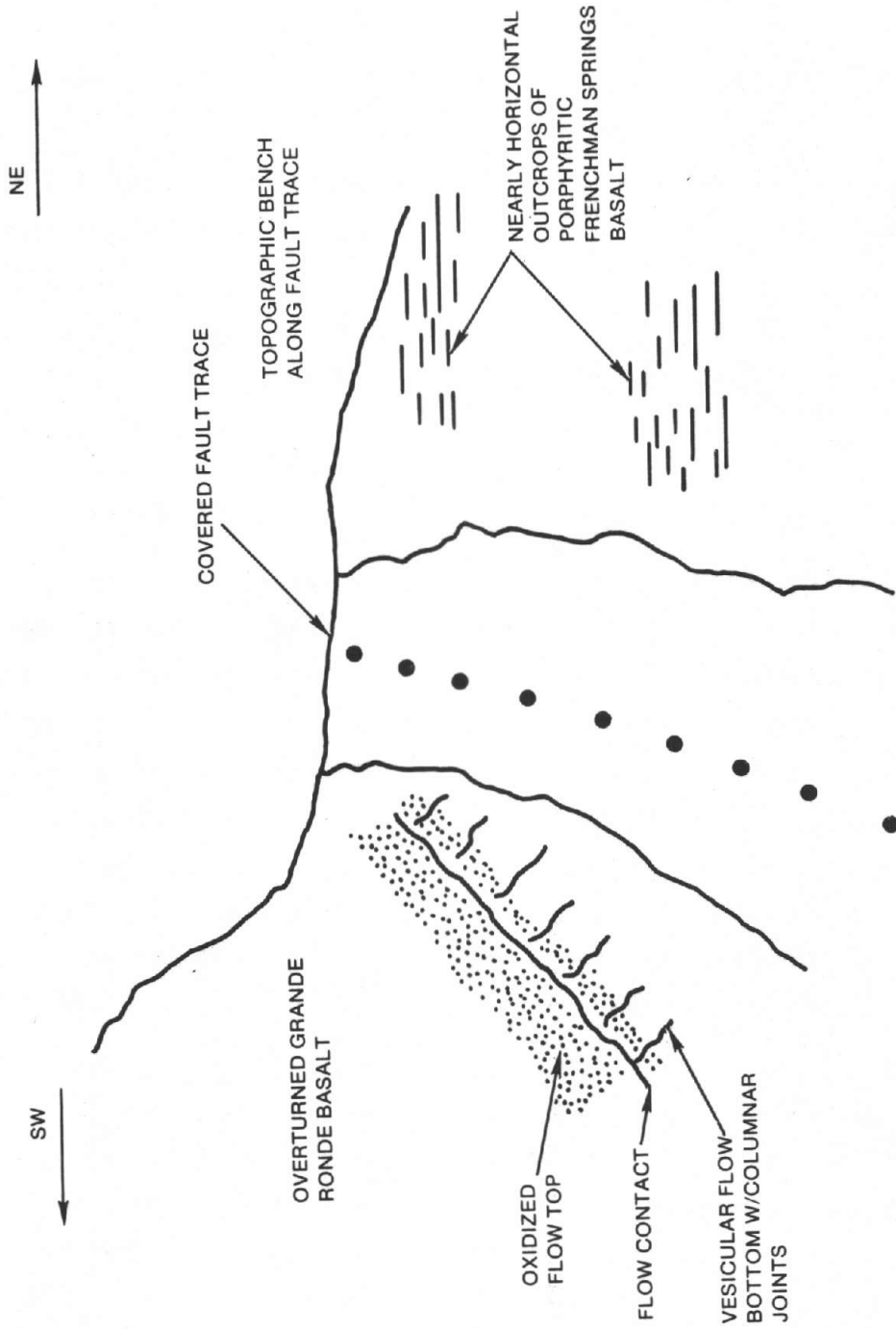
UMTANUM REVERSE FAULT

The Umtanum reverse fault was described by Mackin (1955) in his report regarding the geology around the Priest Rapids Dam site. The fault plane is covered by colluvium and alluvium throughout most of the map area (Figure 25). The basalt units underlying Priest Rapids Dam are nearly horizontal Priest Rapids flows; whereas, southwest of the fault trace, the flows are vertical to overturned Grande Ronde units. Core taken from drill hole PRR-6, located on the buried fault trace, contains several thick zones of gouge and breccia (Mackin, 1955).

The stratigraphic offset produced by the reverse fault is exposed along the south edge of Sec. 33, T14N, R23E (Figure 26) in a gully bounding the north side of a large landslide block. At this location, nearly horizontal, porphyritic Frenchman Springs lavas (Sample C2110, Table 3) on the northeast side of the fault are brought into position against upper Grande Ronde flows (Sample C2111, Table 3) on the southwest side. The attitude of the primary basalt structures indicates the Grande Ronde units are overturned and are dipping 40 degrees to the southwest. Although the actual fault plane is covered, the outcrop appearance and the curvature of the fault contact on the ridge northwest of this gully indicate the fault plane dips about 70 degrees southwest.



FIGURE 25. Vertical Basalt Strata Southwest of Priest Rapids Dam. The Umtanum reverse fault (dotted line) is interpreted to parallel the strike of these strata beneath a cover of alluvium. View is to the east, toward the McCoy Canyon slide complex.



RCP8006-330

FIGURE 26. Sketch of Contact Relationships Adjacent to Umtanum Fault. The fault is exposed on the north side of a gully; south edge of Sec. 33, T14N, R33E.

West of the exposure in the above-mentioned gully, a chaotically deformed mass of porphyritic Frenchman Springs lavas has been thrust over overturned Grande Ronde flows (south Sec. 32 and 33, T14N, R23E). This overthrust mass continues to the northwest beyond Filey Road, indicating it is a major structural feature. The chaotic nature of this area suggests that multiple thrusts have resulted from extreme folding in this portion of the Umtanum anticline.

One normal fault brings deformed Frenchman Springs and Priest Rapids flows into contact with the relatively undeformed Pomona Member and, because of the many observed faults, the Umtanum fault should probably be considered a fault zone.

The Umtanum fault is inferred to be north of the overturned and vertical basalt strata along the face of eastern Umtanum Ridge (Figure 25).

MECHANISM OF FOLDING OF THE UMTANUM ANTICLINE - AN INTERPRETATION

Processes which cause flexural slip in parallel folds, shear zones, zones of reverse faulting, and multiple thrusts, and the existence of a major reverse fault at the margin of vertical strata are evidence that suggest compressional forces in the crust of the earth. The compression was apparently oriented north-south and southwest-northeast, perpendicular to the axis of the Umtanum anticline. Fault plane solutions for microearthquake activity in the Pasco Basin region indicate north- to north-20-degree-west compressional orientations (Suppe and Others, 1975). However, the true orientation of the compressive stress field cannot be evaluated from this mapping study.

On the basis of the data reported here, it seems unlikely that the Umtanum anticline was produced by draping of basalt flows over a deep-seated normal fault (e.g., Bentley, 1977), because this would require well over 500 meters of extension in rocks that exhibit brittle, not ductile, behavior under low temperatures and confining pressure. If the basalt strata were stretched over such a block fault, they would display considerable thinning. Instead, the strata are locally thickened (Figure 13) and compression has caused local zones of multiple thrusts.

AGE OF FOLDING OF UMTANUM RIDGE

Several features suggest that folding of Umtanum Ridge had begun before eruption (14 million years ago) of flows of the Umatilla Member. The dip of the Umatilla is slightly less than the dip of underlying Wanapum lavas exposed on the south flank of the ridge (Figure 27) and there is evidence of thickening of the Umatilla near the Cold Creek syncline. The Umatilla is extensively pillowed in the vicinity of the Cold Creek syncline, suggesting that water had accumulated in the evolving synclinal basin. In addition, the Mabton interbed, which underlies the Umatilla Member, thins onto the south limb of the Umtanum anticline. The Umatilla does not crop out on the north side of eastern Umtanum Ridge or in Sentinel Gap 24 kilometers to the north, suggesting that the developing anticline could have formed a barrier to northward flow of this member. This last argument only applies north of the map area, because the anticline plunges eastward and outcrops of Umatilla on the extreme eastward end of the ridge and in the Gable Butte area show that the Umatilla flowed around the plunging anticline and into an ancestral Pasco Basin.

However, even in Umatilla time, eastern Umtanum Ridge could not have had much more than 100 meters of maximum relief, because the younger Huntzinger intracanyon flow crops out on both sides of the anticline. There is presently a Huntzinger outcrop elevation difference of 600 meters from one side of the anticline to the other (Goff and Myers, 1978). The major stages of folding, faulting, and shearing must, therefore, be post-Huntzinger and probably are post-Pomona in age (based on similar lines of argument).

A minimum age of folding and thrusting could not be determined in the field. No offset of Quaternary deposits was observed. The Umtanum anticline is apparently older than the deformation zone coincident with the Olympic-Wallowa Lineament as discussed below.

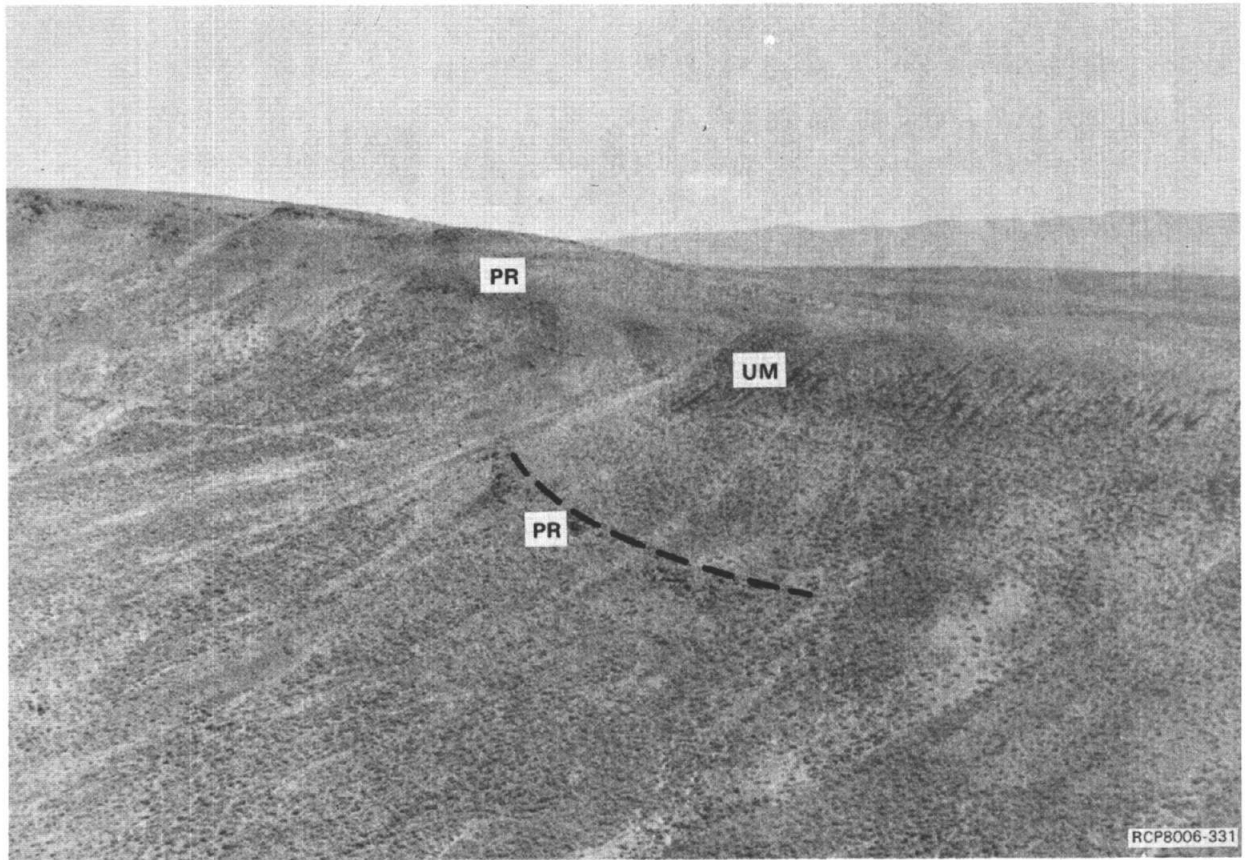


FIGURE 27. Contact Relationships Between Umatilla and Priest Rapids Members. The Priest Rapids Member (Pr) dips more steeply toward the Cold Creek syncline (south, to the right of the field of view) than does Umatilla (Um). The ridge at the left side of the photo is composed of Priest Rapids, and was probably a topographic high in Umatilla time. View is to the northeast, toward the Saddle Mountains (in background). Center Sec. 21, T13N, R24E.

EASTWARD EXTENSION OF THE UMTANUM STRUCTURE

The Umtanum anticline plunges gently eastward beneath the Pasco Basin and forms a linear-positive gravity anomaly that bends southward under the 200 East Area of the Hanford Site (Deju and Richard, 1975; Lillie, 1977). Gable Mountain and Gable Butte appear to be subordinate structures, possibly en echelon folds, associated with the major fold.

Presumably, the monocline, shear zones, and reverse fault on the north limb of the fold extend eastward beneath the Hanford Site as well, although there is some suggestion that shearing lessens in intensity to the east. The gravity gradient over the buried north limb of the fold is not large, indicating that a large topographic escarpment (such as is present west of Priest Rapids Dam) is not present. Therefore, it cannot be determined from this study whether the reverse fault continues uninterrupted, merges into a tight fold axis, splays into other faults (or folds?), or is cut off by another structure. This last suggestion seems to be the least likely and it is suggested here that a zone of sheared rock may exist on the north limb of the buried fold.

OLYMPIC-WALLOWA LINEAMENT

The Olympic-Wallowa Lineament was first described by Raisz (1945), who noted the aligned topography that stretches across south-central Washington. The Olympic-Wallowa Lineament is coincident with the Rattlesnake Hills southeast of Umtanum Ridge. The surface expression of the Olympic-Wallowa Lineament is vaguely defined on eastern Umtanum Ridge, but it can be observed on aerial photographs as a series of northwest-trending lineaments that cross the ridge and straddle Emerson Nipple.

Field mapping of these lineaments was hindered because of the pervasive cover of loess on southern slopes. However, a set of at least four northwest-trending faults or probable faults has caused a linear topography to develop and has offset lithologic units in Sec. 19 and 20 T13N, R24E. In addition, a zone of sheared and brecciated rock (Samples C2046, C2056, and C2069, Table 4) crops out west-northwest of Emerson Nipple and trends across the crest of the ridge into a sharply defined,

northwest-trending gully that exposes the axis of a small but tight fold (Sec. 13, T13N, R23E). Another small fold appears in the next gully to the northwest.

The most significant deformation that might be attributed to the Olympic-Wallowa Lineament is the apparent left-lateral displacement of the Umtanum anticlinal hinge at the McCoy Canyon block slide (Plate 1). This slide complex breaks the continuity of the anticline for a distance of about 2 kilometers. The crest of the anticline bends southeast as it enters the western edge of the slide complex and bends northwest as it enters the eastern edge. Projection of the crest line to a common northwest-trending reference line (representing the Olympic-Wallowa Lineament) suggests left-lateral displacement of roughly 1 kilometer and indicates movement after the formation of the Umtanum anticline.

The Olympic-Wallowa Lineament is best described as a deformation zone consisting of short faults, tight folds, and cataclastically deformed rocks. No evidence for Quaternary movement was found, but it must be remembered that the only Quaternary sediments covering these structures on eastern Umtanum Ridge are loess and colluvium. Elsewhere along the margin of the Pasco Basin, the Olympic-Wallowa Lineament is associated with normal and reverse faults reflected by sharply defined linear topography, but assignment of a Quaternary age to these features is unsupported (Gardner, 1977; Jones and Fecht, 1977).

FOLDING SOUTH OF UMTANUM RIDGE

The period of folding that produced Umtanum Ridge is also responsible for the major topographic feature just to the south. Cold Creek essentially follows a synclinal axis between Umtanum and Yakima Ridges. South of Cold Creek, the structure is more complicated. The general structural configuration there is that of a second major anticlinal axis near the crest of Yakima Ridge. However, a short, prominent ridge between Cold Creek Valley and Yakima Ridge (Sec. 26, T13N, R23E) represents a third anticline less than 2 kilometers long. This third anticline rises sharply south of a low cliff bordering a very straight segment of Cold Creek (NE 1/4, Sec. 26, T13N, R23E), which is the topographic expression of a second monocline.

The second monocline is easily visible from the road across Cold Creek because of the steeply dipping, fractured rocks that comprise the cliff. A narrow zone of sheared rock is parallel to and southwest of the monocline axis, but it can be observed only beneath the rubble covering the sides of deep gullies that cut across the monocline. This monocline could possibly represent an immature stage in the evolution of a monocline similar to that described on eastern Umtanum Ridge. The geometrical resemblance of the two anticlines and monoclines is noteworthy and suggests that the mechanism of folding that produced Umtanum Ridge also created Yakima Ridge.

NORMAL FAULTS

Many normal faults of short length and minor displacement were found in the map area. These were recognized on the basis of offset units, linear topography (such as ridge lines and stream drainages), and the positions of springs. The actual fault planes are generally covered, and gouge and/or breccia are rarely found. The existence of many of these faults is questionable, and evidence for their presence is scanty. Most of these faults have a north to northeast trend, which is perpendicular to the attitude of the fold axes, and it is my opinion that these faults represent minor, near-surface, crustal adjustments contemporaneous to or later than the folding. No evidence of Quaternary movement was found for any of these faults. Three of these faults are discussed below.

A covered, northeast-trending fault runs beneath the landslide complex at Juniper Springs and brings the upper porphyritic Frenchman Springs unit into stratigraphic adjacency with the lower porphyritic unit. The Vantage Member, which crops out as a thick sandstone interbed 0.5 kilometer west of the exposed fault trace, does not appear east of the fault trace or slide complex.

A conspicuous north-northeast-trending fault runs through a deep swale and follows a linear canyon down the north face of eastern Umtanum Ridge (NW 1/4, Sec. 14 and 11, T13N, R23E). This fault offsets the Vantage and MgO horizons farther downslope.

The presence of a north-trending pair of possibly continuous faults on Yakima Ridge (Sec. 26 and 35, T13N, R23E) is strongly implied by abrupt changes in elevation of Priest Rapids and Frenchman Springs flows on either side of the proposed fault trace.

AERIAL PHOTOGRAPHIC LINEAMENTS

Two prominent pairs of northeast-trending, aerial photographic lineaments cross the Umtanum anticline on the east end of the map area, but no evidence of faulting was found in association with them. The west pair traverses the east margin of the Juniper Springs slide complex; the west lineament of this pair is defined, in part, by a closed topographic depression behind a large block slide (Figure 28). The east lineament of this pair follows a straight gully down the flank of the ridge and over a cliff, through large fractures (joints) in the Frenchman Springs Member.

The east pair of lineaments is defined by topographic benches and aligned gullies in outcrops of the Pomona and Umatilla (Figure 29). This pair may have been produced by rapid erosion of the plunging anticline during periods of glaciofluvial flooding, but the parallelism of these and other lineaments to the system of northeast-trending faults suggests the lineaments are structurally controlled.

INTRACANYON STRUCTURE

The Wahluke and Huntzinger lavas flowed through a northeast-trending paleovalley across Umtanum and Yakima Ridges (Figure 3). The outcrop pattern of the Wahluke flow is strikingly linear and it is probable that the ancient stream cut its course in a northeast-trending structure. The basalt in this area is deeply eroded and extensively folded. No evidence for faulting was found; however, the structure is most probably a fracture or system of fractures (joints) related to the other northeast-trending linear structures.

LANDSLIDES

Small landslides occur on steep slopes throughout the map area; most of them are tongues of debris that moved chaotically downslope. Many of

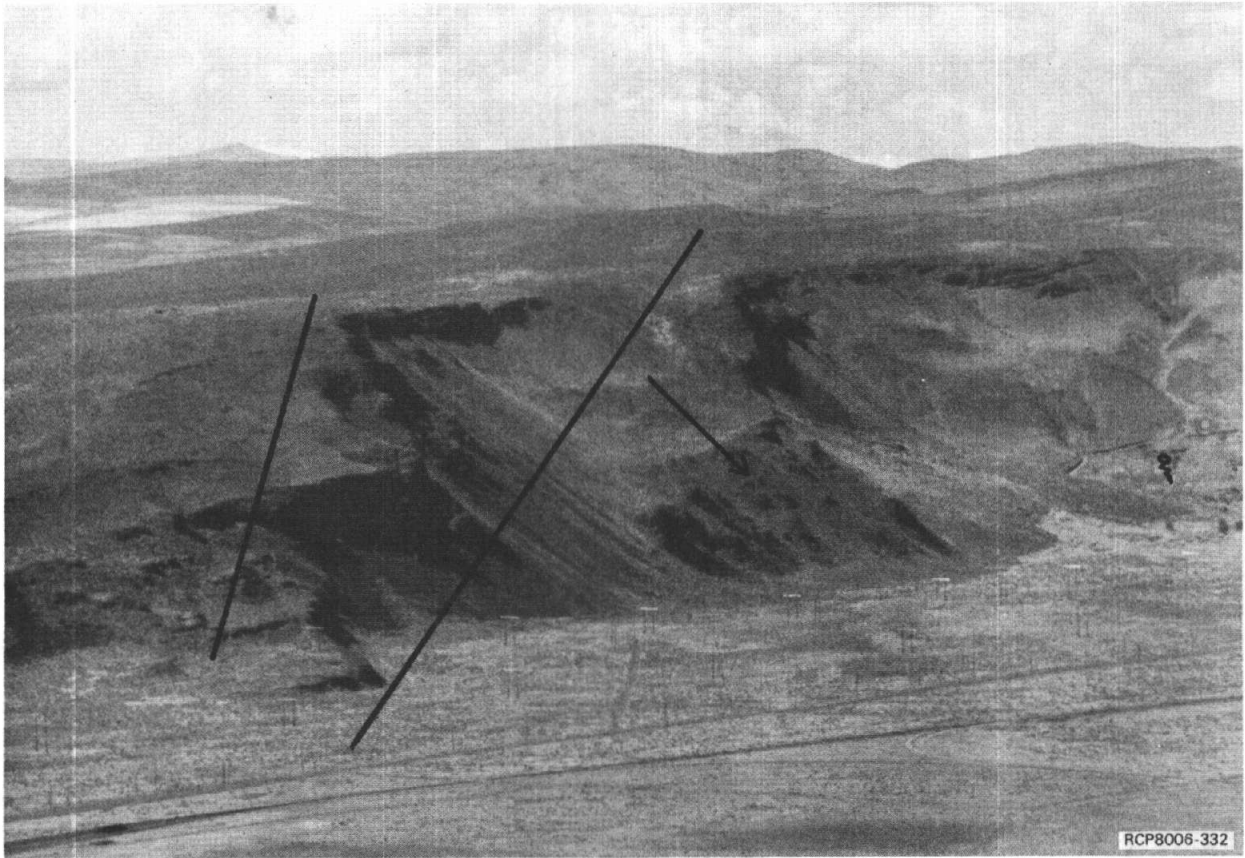


FIGURE 28. Juniper Springs Slide Complex. Juniper Springs issues from the vegetation at right (west) side of the field of view. A large slide block is downdropped to the northwest (in direction of arrow). Straight lines mark the approximate trace of lineaments visible on air photos. View is to the southwest.

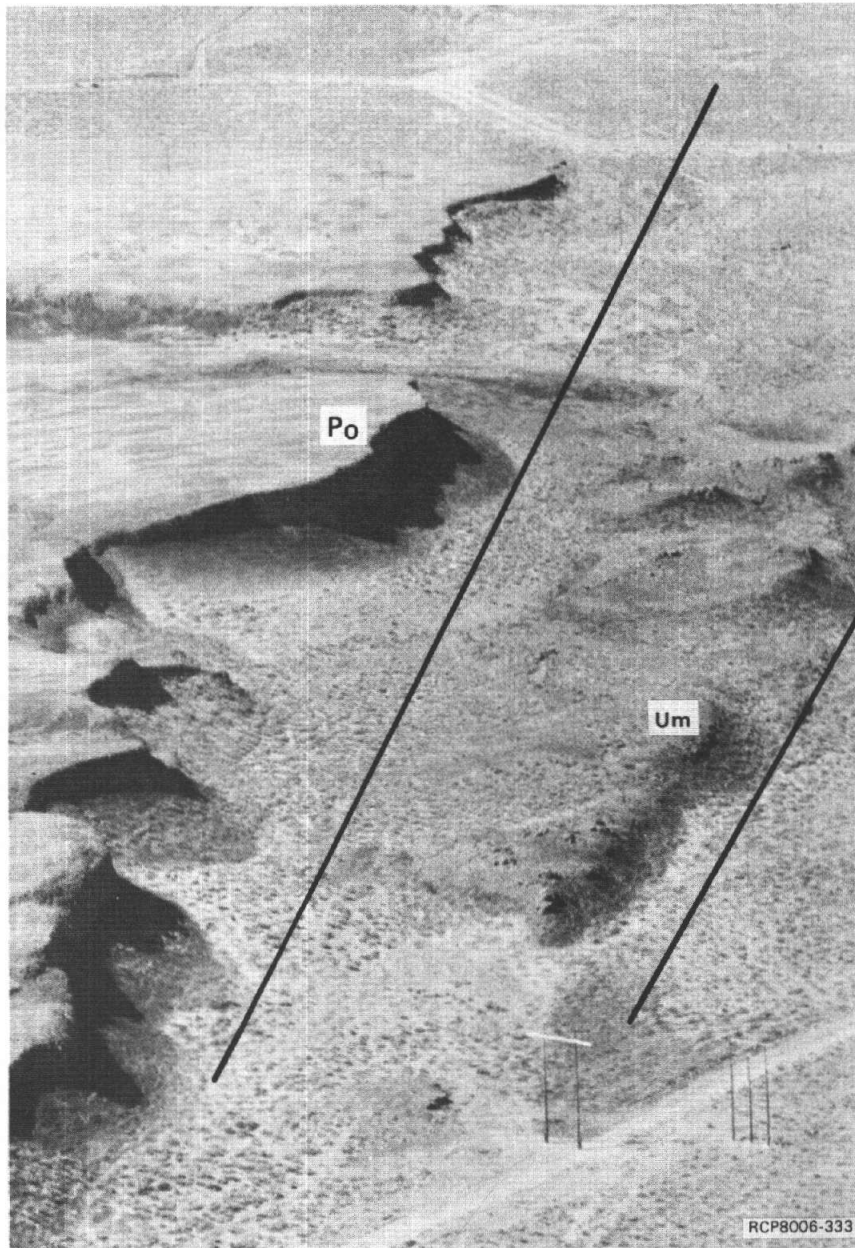


FIGURE 29. Lineaments Visible on Areal Photographs. The photograph shows the traces (inked lines) of lineaments visible on areal photographs. Topographic benches have been eroded into the Pomona (Po) and Umatilla (Um) Members. View to the southwest. Sec. 17, T13N, R25E.

the slides were caused in part by over-steepening of the slope and slippage of basalt along contacts with relatively incompetent interbeds, such as the Mabton.

In contrast to these small, thin, landslide deposits, two areas of extensive block sliding modify the topography along the north face of eastern Umtanum Ridge; the McCoy Canyon landslide complex and the Juniper Springs landslide complex. It is suggested that these slides are caused, in part, by intersections of major structures that weaken the rocks and, in part, by rapid erosion at the toe areas by the Columbia River. Continued movement in these slide complexes is possible.

McCOY CANYON SLIDE COMPLEX

The McCoy Canyon area consists of roughly 3 square kilometers of slide blocks (Tereva blocks) and smaller chaotic slides (Figure 30). The major block is adjacent to the Columbia River and exposes about 350 meters of basalt section. The slide complex is clearly defined by the 3-kilometer-long arcuate headwall zone carved into the ridge and by the nearly closed topographic depression behind the slide blocks. Mapping along the east margin of this block shows that the Vantage horizon has dropped 170 meters and that the basalt strata have rotated such that they dip 10 degrees more steeply to the south than do adjacent, in-place strata to the east. The continuity of the anticlinal hinge is broken at this point as well. In the prominent topographic bend midway down McCoy Canyon, the Vantage horizon appears as two deformed outcrops with chaotic dips. Two smaller slide blocks are stacked against the southwest edge of the major block.

Smaller debris slides and colluvium are draped across the headwall zone of the slide complex. The entire basin behind the slide blocks is covered with loess, but it is conceivable that lenses of glaciofluvial sediments are hidden beneath this cover. Arcuate stream drainages outline the slide masses throughout the slide complex.

Despite this evidence, Converse, Davis and Associates (1970) concluded that the bowl-shaped topography behind the slide blocks

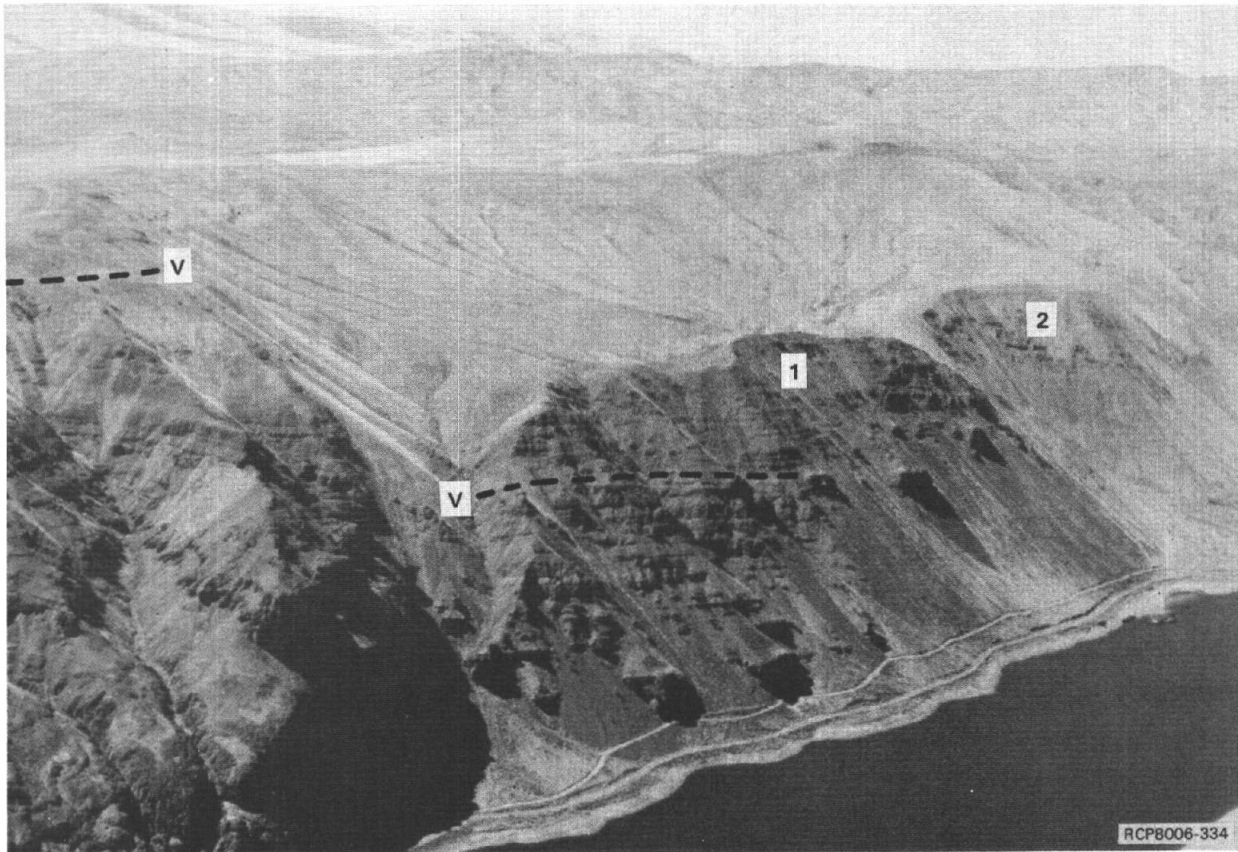


FIGURE 30. McCoy Canyon Slide Complex. Note the arcuate headwall zone behind and above the two largest slide blocks (numbered 1 and 2 on the photo). The Vantage horizon (V) is shown by a dashed line. View looking southwest, across the Columbia River.

resulted from fluvial or glaciofluvial erosion and that the major block slide resulted from either faulting or complex folding. The distinction between fault blocks and large slide blocks can be very difficult to discern, particularly if headwall scarps do not extend beyond the down-dropped masses (Goff and McLaughlin, 1976), but slide blocks move downslope along slide planes which are inclined from the horizontal. The base of the slide plane beneath the major McCoy Canyon slide block is exposed as a prominent bench of fractured lower Grande Ronde (Schwana sequence) Basalt (Samples C2099 and C2100, Table 3) that is continuous with similar rocks in the shear zone east of the slide block (Figure 31). This bench was probably cut by the Columbia River prior to landsliding.

The position of the McCoy Canyon slide complex at the intersection of the Umtanum anticline and the Olympic-Wallowa Lineament is noteworthy and it is speculated that tectonic weakening of basalt units at this intersection has greatly enhanced the slide potential.

JUNIPER SPRINGS SLIDE COMPLEX

A 1.5-kilometer-wide arcuate embayment is carved out of eastern Umtanum Ridge at Juniper Springs (Figure 28). This embayment is partially filled with one large slide block and many chaotic slides which form discrete tongues of jumbled rock. Much of the sliding appears to be related to the incompetent Vantage horizon on the west side of the slide complex. However, the major cause of sliding is probably due to the intersection of the northeast-trending fault and lineaments with the Umtanum anticline. This intersection has possibly reduced the competency of the basalt strata.

WATER QUALITY AND GEOTHERMAL POTENTIAL

Four artesian wells in the southeast part of the map area discharge water which is slightly warmer than the ambient air temperature of the region. These wells were drilled through alluvium into basalt bedrock and lie along the postulated covered southeast extension of the projected Olympic-Wallowa Lineament as it crosses eastern Umtanum Ridge. The

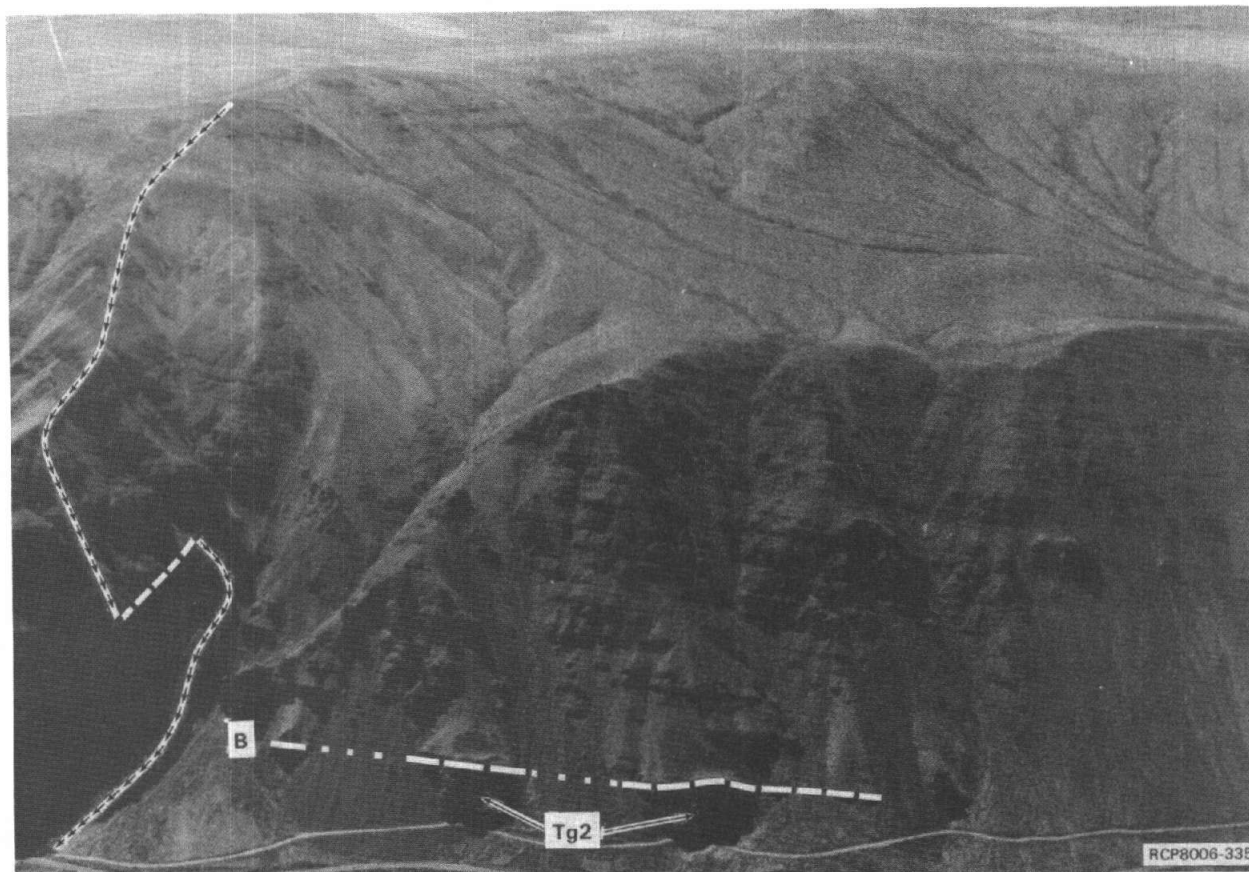


FIGURE 31. Major Slide Block, McCoy Canyon. The base of the slide plane appears as a topographic bench (B, Schwana surface) composed of sheared lower Grande Ronde Basalt (Ts) which is stratigraphically continuous with similar sheared rocks to the east (left) of the slide block. The measurement traverse of the stratigraphic section (Plate 2) is shown on this figure by a chevron pattern. View looking south.

chemistry of selected waters from these wells and from other springs and wells in surrounding areas was interpreted in order to assess the source of the artesian water and its relationship to the Olympic-Wallowa Lineament.

Samples were collected in mid-summer of 1977. Few easily accessible springs, untrampled by cattle, flow from eastern Umtanum Ridge during this season. Waters from four cold springs in the Rattlesnake Ridge region were collected with the help of Mr. J. N. Gardner and Mr. M. Neese to establish background chemical conditions. The other samples were comprised of waters from two artesian wells (one of which is shown in Figure 32), one deep irrigation well (courtesy of Mr. D. Wilson, St. Michelle Vintners), and Juniper Springs on the north face of eastern Umtanum Ridge. Three of the springs are associated with obvious landslide zones.

The water chemistry and pH of all eight samples (Table 7) are strikingly similar, although they issue from a variety of depths and geologic settings. The waters are dilute and of good drinking quality. They can be divided into two subtly different chemical groups which correlate with the areas (coincidentally) from which they were collected. The cold surficial waters, Samples PBS-1 to PBS-4 (Group A) contain less SiO_2 , Na^+ and K^+ than the other four waters sampled (Group B). The close similarity of Juniper Springs waters to the well waters of Group B suggests that some aquifer may be common to all.

Juniper Springs issues from the Juniper Springs landslide complex that covers a probable fault. The most obvious aquifer that might supply the spring (if it is not merely a landslide spring) is the Vantage sandstone interbed which crops out 770 meters to the east. Many springs issue from the Vantage sandstone on the north face of eastern Umtanum Ridge. To test the hypothesis of a common aquifer, a calculation was made to roughly estimate depth to the Vantage sandstone beneath a well with a known depth of water entry. St. Michelle Well #2 encounters a large water entry at approximately the 245-meter depth. The well head is at an approximate elevation of 338 meters. The nearest exposed Vantage horizon crops out 3,385 meters due north of this well at an elevation of

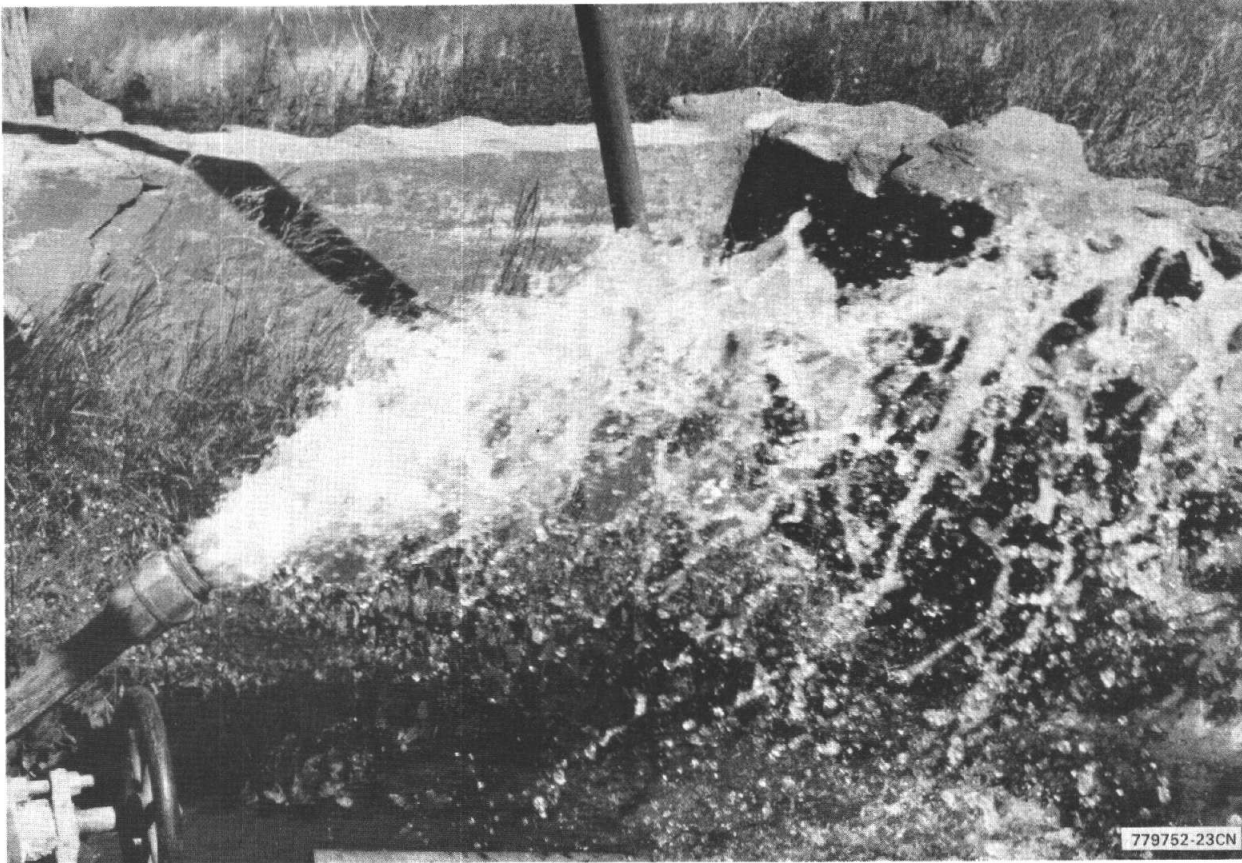


FIGURE 32. Artesian Well #1. Gate valve fully open. Although this water is relatively warm (22°C), it contains few solutes.

400 meters on the Umtanum anticlinal axis. If we assume an average constant Vantage horizon dip of 5 degrees south, then the elevation of the Vantage beneath the collar of St. Michelle Well #2 is calculated at 101.5 meters (Figure 33). The estimated depth to water entry is then 234 meters, which agrees well with the recorded depth of 245 meters. This calculation ignores any complications caused by offset along the Juniper Springs fault. Even so, it suggests that the probable source aquifer of St. Michelle Well #2 is the Vantage horizon or overlying Frenchman Springs basalt.

According to Mr. D. Leitch (Washington State Highway Department), the flow of artesian well #1 was cut in half shortly after St. Michelle Well #2 was drilled in 1974. This fact, in combination with the similar chemistry of Group B waters, argues that all four Group B waters originate in part from the same horizon. The relatively higher Na^+ and K^+ of these waters probably results from reactions with feldspars and micas which are plentiful in the Vantage sandstone. The slightly higher SiO_2 probably results from a longer residence time of the water in the source aquifer, as compared with the residence times of cold surficial waters. Group B waters may have higher temperatures because the source aquifer is buried up to 325 meters or more below the ground surface. The temperatures of Group B waters increase as the well locations are positioned progressively down-dip on the Umtanum anticline.

The slight differences in chemistry of the two water types are reflected in the subsurface equilibration temperatures estimated from the Na-K-Ca geothermometer of Fournier and Truesdell (1973). Group A surficial waters average about 40°C less in estimated subsurface temperature than Group B aquifer waters, although within each group waters of higher measured temperature generally yield higher estimated equilibration temperatures.

The calculated subsurface equilibrium ($\text{Beta} = 4/3$) temperatures of Group B waters are more than 25°C above their measured temperatures (see Table 7). This suggests that there may be minor subsurface mixing of a deeper warm water with cold meteoric water (Fournier and Truesdell, 1974). If such deep water exists, it may rise along the Juniper Springs

TABLE 7. Temperatures, Flow Rates, and Chemical Analyses of Eight Spring and Well Waters From Rattlesnake and Eastern Ridge Region Collected and Analyzed in July-August 1977*

SAMPLE NUMBER	PBS-1	PBS-2	PBS-3
SAMPLE NAME	RATTLESNAKE SPRINGS	MIDDLE SNIVELY SPRINGS	BENNETT SPRINGS
GROUP	A	A	A
LOCATION	North 1/2, Sec. 29 T12N, R25E	Center, Sec. 8 T11N, R25E	Center, Sec. 14, T11N, R24E
Temp. °F (°C)	63 (17)	59 (15)	56 (13)
Flow rate (gpm)	5-10	2	1.5
Field pH**	5.6	5.9	5.8
SiO ₂	45	40	50
Mg ²⁺	10.0	7.5	7.7
Ca ²⁺	25.5	17.5	20.0
Na ⁺	13.0	7.5	8.0
K ⁺	4.0	2.5	2.3
Li ⁺	0.1	0.1	0.1
Fe (Total)	0.1	0.1	0.1
HCO ⁻	123	83	83
SO ₄ ²⁻	4.5	3.5	4.0
Cl ⁻	4.5	4.5	7.25
F ⁻	0.46	0.3	0.28
B	0.1	0.1	0.1
Na-K-Ca Geothermometer, Beta = 4/3, °C	45	34	31
Comments	Issues from Dry Creek south of possible fault scarp on Yakima Ridge.	Flows from stream gully by old ranch house in large land- slide complex.	Three springs at head of land- slide; collected and piped to pond.

*All species reported in parts per million.

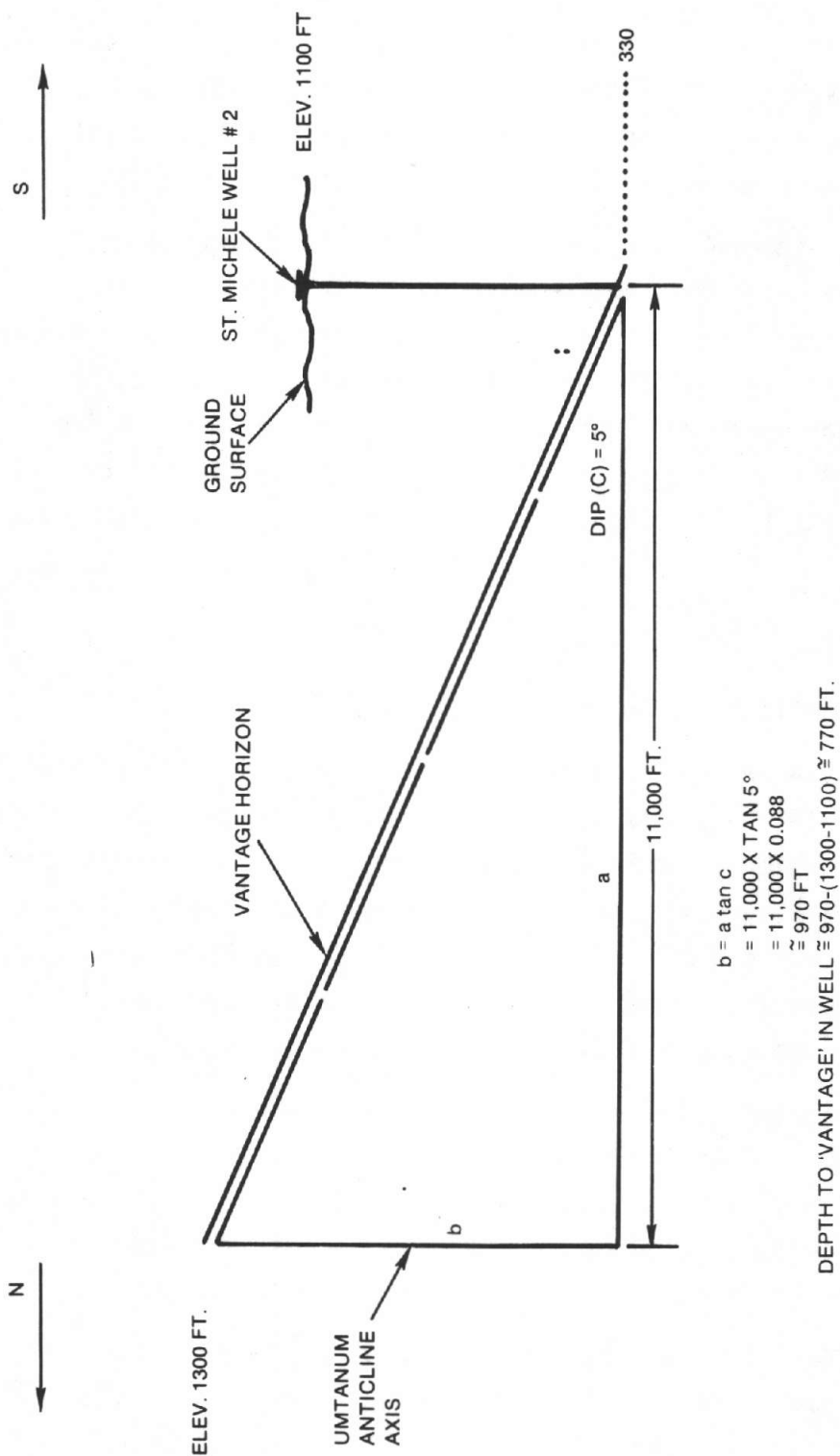
**Colorphast pH indicator strips numbers 9581, 9582, and 9583.

Table 7 (continued)

SAMPLE NUMBER	PBS-4	PBS-5	PBS-6
SAMPLE NAME	MAIDEN SPRINGS	ARTESIAN WELL # 1	MAGEE WELL
GROUP	A	B	B
LOCATION	East 1/2 , Sec. 18 T11N, R24E	NW 1/4, Sec. 30 T13N, R124E	Center, Sec. 14 T13N, R25E
Temp. °F (°C)	56 (13)	73 (23)	81 (27)
Flow Rate, gpm	1.5	300	500
Field pH**	5.7	6.0	5.9
SiO ₂	30	55	60
Mg ²⁺	6.0	7.0	7.7
Ca ²⁺	15.0	15.0	14.0
Na ⁺	7.0	21.0	24.0
K ⁺	1.8	7.0	8.5
Li ⁺	0.1	0.1	0.1
Fe (Total)	0.1	0.1	0.15
HCO ⁻	72	144	141
SO ₄ ²⁻	2.5	0.5	0.5
Cl ⁻	3.75	5.0	4.25
F ⁻	0.22	0.72	0.76
B	0.1	0.1	0.1
Na-K-Ca Geothermometer B = 4.3, °C	28	76	86
Comments	Issues from alluvium at mouth of gully	Well drilled through alluvium into basalt; 20.3-centimeter iron casing; depth to water entry unknown	Well drilled through alluvium into basalt; 30.5-centimeter iron casing; depth to water entry unknown

Table 7 (continued)

SAMPLE NUMBER	PBS-7	PBS-8
SAMPLE NAME	JUNIPER SPRINGS	ST. MICHELLE WELL
GROUP	B	B
LOCATION	Center, Sec. 14, T13N, R24E	Center, Sec. 27, T13N, R24E
Temp. °F (°C)	64 (18)	69 (21)
Flow rate, gpm	10	500
Field pH**	5.9	6.7
SiO ₂	55	55
Mg ²⁺	13.3	10.8
Ca ²⁺	19.5	16.5
Na ⁺	20.5	21.0
K ⁺	6.25	6.5
Li ⁺	0.1	0.1
Fe (Total)	0.15	0.15
HCO ⁻	148	144
SO ₄ ²⁻	7.5	0.5
Cl ⁻	5.75	5.0
F ⁻	0.62	0.64
B	0.1	0.1
Na-K-Ca Geothermometer, B = 4/3, °C	67	72
Comments	Flows from base of large block in landslide complex.	Well drilled in alluvium and basalt, 30.5-centimeter iron casing; depth to water entry about 245 meters



RCP8006-336

FIGURE 33. Calculation of Depth to Vantage Interbedded Horizon. St. Michele Well #2.

fault and flow down dip through the source aquifer. However, the waters are relatively cold and dilute and have low concentrations of key elements or ions (e.g., Li^+ , Cl^- , SO_4^{2-} and B) that suggest deep thermal equilibration with an underlying geothermal reservoir (see White, 1957; White and Others, 1973; Goff and Others, 1977). Without the presence of a positive indicator of heat, the geothermal potential beneath eastern Umtanum Ridge is considered to be nil.

The apparent association of artesian wells with the postulated location of the Olympic-Wallowa Lineament suggests that the Vantage horizon may locally be over-pressured in this deformation zone. Another logical explanation is that the artesian wells get their hydraulic head from a high elevation of recharge on the source aquifer west of the wells. Both hypotheses require detailed hydrologic testing of the artesian and adjacent non-artesian wells to resolve remaining questions.

RECOMMENDATIONS

WASTE REPOSITORY SITE AND HYDROLOGIC CONSIDERATIONS

Should a nuclear waste repository be established, it will probably contain nuclear waste whose solubility in water is minimal. Nonetheless, groundwater might slowly leach potentially harmful radionuclides if it can gain entrance to repository caverns. It is recommended that the proposed nuclear waste repository be located away from fault zones, shear zones, and areas of fractured rock that might promote groundwater circulation into the caverns should they somehow be ruptured.

Therefore, the proposed repository should not be located near the buried north flank of eastern Umtanum Ridge or on the associated east-west-trending zone of sheared rocks. It may be difficult to predict the location of buried, north-trending faults such as occur on eastern Umtanum Ridge because their distribution appears to be random.

The thick Umtanum basalt flow and similar flows above and below, which are being considered as proposed repository host rocks, display some of the most intense deformation exposed on eastern Umtanum Ridge (Figure 16). Away from the shear zones, however, these flows are

probably much less disturbed. Circulation of deep groundwater through primary flow structures such as cooling joints or pillow zones may to some extent be unavoidable. However, the major avenues of movement for circulating groundwater within the buried, south flank of eastern Umtanum Ridge are probably at or near the flow contacts and interbed horizons such as the Vantage sandstone.

As possible aids to interpretation of the detailed structure beneath the Hanford Site, the following is recommended:

1. Detailed seismic surveys crossing perpendicular to the projected concealed extension of the Umtanum reverse fault and shear zones. These surveys might reveal with greater clarity major structural lineaments or offset of strata associated with the reverse fault which gravity studies do not show.
2. Small-diameter core holes over sites of possible shearing in the buried north flank of the anticline to verify the presence or absence of cataclastic rocks; these sites should be chosen with the aid of geophysical surveys.
3. Small-diameter core holes surrounding sites selected for further evaluation as repositories. The stratigraphy revealed by these cores may indicate faults or other structures in the site vicinity.

SEISMIC CONSIDERATIONS

The structure considered to have the most potential for seismic activity is the deformation zone coincident with the postulated Olympic-Wallowa Lineament; however, no evidence for Quaternary movement was found along this zone on eastern Umtanum Ridge. Possible studies might include the following.

1. Seismic surveys to define buried topographic lineaments that may be associated with the Olympic-Wallowa Lineament.
2. Trenches across significant lineaments found by field mapping or geophysical surveys. Preferably, trenches would be excavated where possible deformation could be observed in overlying glaciofluvial or

other young sediments. Possible locations might be in the notch between Wahluke outcrops just southwest of Emerson Nipple and near the extreme east end of Yakima Ridge, where a linear escarpment of the Elephant Mountain Member was reconnaissance mapped.

3. Detailed study of the drill cores taken during construction of Priest Rapids Dam. According to Mackin (1955), several faults are suggested by the stratigraphic relations in these cores and the dam site lies astride the northwest extension of the Olympic-Wallowa Lineament as it crosses eastern Umtanum Ridge.

GENERAL RECOMMENDATIONS

1. A detailed magnetic survey should be run through the basalt section described on Plate 2 to determine magnetic polarities, inclinations, and declinations. This survey would check the stratigraphic correlation application of a similar traverse conducted by Coe and Others (1978) at Sentinel Gap.
2. A detailed study of the genesis of thick flow-top breccias should be undertaken to better understand the intraflow structures in flows which may house nuclear waste.
3. A second stratigraphic section should be measured in the canyon described in Figure 6 in order to compare stratigraphic variations in the Grande Ronde Basalt.
4. The thrust faults and compressive stress field of the Umtanum fault and anticline should be studied in detail to understand the mechanisms and style of similar structures throughout the Pasco Basin.
5. The Priest Rapids interbed discovered on Yakima Ridge should be studied to see if it represents a significant time interval between Priest Rapids and Lolo chemical types.
6. The paleomagnetism and chemistry of the "Roza-like" porphyritic flows mapped on Umtanum and Yakima Ridges should be studied to determine if they are the Roza Member of Mackin (1955).

CONCLUSIONS

Geologic mapping, whole-rock chemistry, and natural remanent magnetic polarities show that eastern Umtanum Ridge is an asymmetric anticline formed by folding of over 20 layers of Columbia River basalt. This folding began before Umatilla time (14 million years ago) and probably continued well beyond Pomona time (10.5 million years ago), culminating in the formation of the Umtanum reverse fault. Mapping aided by petrographic and X-ray diffraction studies show that the fault is associated with fractured rock and shear zones which probably extend eastward beneath the Hanford Site. Some normal faults cut the basalt members on eastern Umtanum Ridge suggesting that other normal faults may lie buried beneath the Hanford Site. The faults, fractures, and shear zones may act as local corridors for the movement of groundwater. Similar structures beneath the Hanford Site can and should be avoided in the construction of proposed nuclear waste repositories.

The Umtanum structures are older than geologic structures coincident with the Olympic-Wallowa Lineament. As of yet, no conclusive evidence has been found to suggest this lineament is an active fault zone.

APPENDIX
DESCRIPTION OF MAP UNITS

NOTE: Descriptions are in order of increasing age. Potassium/argon ages are for whole-rock samples and were obtained from ARH-ST-137 (1976) unless otherwise noted.

- Qa ALLUVIUM -- River and stream deposits of conglomerate, sand, silt, and clay which fill present-day valleys; maximum thickness in Cold Creek Valley is less than 5 meters; maximum thickness in Columbia River Valley is unknown.
- Ql LOESS -- Wind-blown dust and silt which blankets gentle slopes; mapped only where no outcrops exist or where covering critical contacts; maximum thickness less than 10 meters.
- Qaf ALLUVIAL FAN DEPOSITS -- Unsorted, coarse, and fine materials deposited at the mouths of small, steep valleys during periods of rapid erosion; maximum thickness about 15 meters.
- Qco COLLUVIUM AND TALUS -- Coarse material and silt derived by downslope movement on steep slopes due to gravity; mapped only where very conspicuous or where covering critical contacts; maximum thickness about 10 meters.
- Qld LANDSLIDES -- Coherent stratigraphic blocks, unsorted rock and soil, or mixtures of both which have moved downslope as units or as a series of units; some slides subject to continued movement; areas of extensive block sliding were mapped at McCoy Canyon and Juniper Springs, respectively; recognized by hummocky topography, closed to nearly closed topographic depressions, bowl-shaped headwall zones, and rotation of dip of bedded units; maximum thickness at McCoy Canyon is on the order of 400 meters; maximum thickness of most slides is less than 30 meters.
- Qag TERRACE GRAVELS -- Rounded to subangular clasts of basaltic gravel in a matrix of sand and silt deposited along ancestral

Cold Creek; includes minor side-stream fan conglomerate; local basaltic sources only; subject to extensive caliche deposition; maximum thickness near mouth of Cold Creek greater than 20 meters; thickness generally less than 5 meters.

- Qhp GLACIOFLUVIAL SEDIMENTS -- Conglomerate, sand, silt, and clay that include clasts of granitic and metamorphic origin; deposited during late Pleistocene catastrophic floods of ancestral Columbia River and Lake Missoula; deposits restricted to east end of map area; occasional large glacial erratics or lenses of conglomerate which are too small to map; maximum thickness in map area 100 meters(?).
- Tp POMONA -- Black to dark grey porphyritic basalt with 1% of plagioclase phenocrysts up to 1 centimeter long which are often sieve-textured; contains 1% of olivine phenocrysts 0.5 millimeter across; olivine commonly altered to orange clays and Fe oxides; occasionally forms dark talus ribbons on steep slopes; generally has narrow colonnade; columns 0.2-0.4 meter across which radiate outward and fan upward; base of flow is extensively pillowed in SE 1/4, Sec. 29, T13N, R24E; consists of two flow units at extreme north tip of outcrop in NW 1/4, Sec. 32, T13N, R24E; overlies rare sediments and tuff of Selah horizon and Umatilla basalt south of Umtanum anticline; overlies Selah tuff and Priest Rapids basalt north of anticline; magnetic polarity reverse; potassium/argon age 10.5 million years; maximum thickness 30 meters.
- Te1 ELLENSBURG (SELAH) -- Grey volcanoclastic sand and silt and rhyolitic ash; upper 0.5 meter of ash locally welded to dark grey perlitic glass by overlying Pomona basalt; ash generally is white and pumaceous, with occasional accretionary lapilli 0.5 centimeter across; only rare lenses of sediment and ash exposed south of Umtanum anticline; extensive white ash deposit is discontinuously exposed north of anticline and west of Priest Rapids Dam on the "Selah Bench;" maximum thickness 20 meters(?).

- Ta HUNTZINGER -- Intracanyon flow of grey to black porphyritic basalt with variable hand-specimen appearance; may be ophitic and diktytaxitic with plagioclase phenocrysts up to 1 centimeter long and olivine up to 0.5 millimeter across enclosed by ophitic pyroxene; glassy samples contain a total of 1% phenocrysts of plagioclase (1 centimeter or less long) and pyroxene and olivine (0.5 millimeter across); hand samples easily confused with Pomona basalt; crops out as prominent black ridge overlying Wahluke basalt in Sec. 24, T13N, R23E; forms conspicuous ledge on north side of Columbia River below Priest Rapids Dam; colonnade columns are thick, up to 1 meter across; entablature forms hackly chunks about 0.2 meter across; minor pillowing exposed at base of flow; top of flow eroded; magnetic polarity normal; potassium/argon age 12.6 ± 0.4 million years (Ward 1976); maximum thickness 40 meters(?).
- Tw WAHLUKE -- Intracanyon flow of black aphyric basalt with conspicuous plagioclase microphenocrysts 1-2 millimeters long and rare plagioclase phenocrysts up to 1 centimeter long; commonly has tiny, pervasively distributed vesicles 0.5-3 millimeters across; has concoidal fracture; hand samples easily confused with Umatilla basalt; outcrops on Emerson Nipple, below Huntzinger basalt on ridge to west, and on top of Yakima Ridge in NW 1/4, Sec. 35, T13N, R23E; primary flow characteristics poorly exposed, but has hackly entablature; minor pillowing at flow base; overlies Priest Rapids and Frenchman Springs basalts (Roza(?) basalt); magnetic polarity normal; potassium/argon age 12.7 million years; maximum thickness 30 meters(?).
- Tu UMATILLA -- Black, glassy, aphyric basalt with abundant plagioclase microphenocrysts less than 0.25 millimeter long; has distinctive concoidal fracture and rare plagioclase phenocrysts; forms dark talus ribbons on steep slopes; colonnade columns vary from 0.3-1 meter across depending on outcrop location; entablature is hackly; flow base is extensively pillowed especially near the Cold Creek syncline; cross-bedding of pillow lobes indicates lava flowed in a west-northwest direction near

ancestral Cold Creek; flow top is poorly exposed; overlies Ellensburg horizon and Priest Rapids basalt; magnetic polarity normal; K/Ar age 14.1 million years; maximum thickness about 50 meters.

- Te1 ELLENSBURG (MABTON) INTERBED -- Discontinuous exposures of buff to brown sandstone, siliceous silt, gravel, chert, and petrified wood; gravel locally cemented with hydrated Fe oxides and contains clasts of chert, granitic rocks, and metamorphic rocks; generally overlies a deeply weathered zone in Priest Rapids basalt; maximum thickness less than 10 meters.
- Tpr PRIEST RAPIDS -- Four and possibly more flows of grey, usually diktytaxitic aphyric basalt with a coarse texture produced by plagioclase microphenocrysts; contains rare plagioclase phenocrysts up to 1.5 centimeters long; outcrops weather to rusty-brown color; colonnade and entablature are broad and diffuse; flow top is coarsely vesicular; some flows or flow units(?) contain vesicle cylinders and vesicle sheets (Goff, 1976 and 1977); flow base is rarely pillowed; uppermost flow is darker, more massive, and finer grained than others; uppermost flow overlies a prominent interbed (Te1) of siliceous siltstone, chert, and petrified wood up to 5 meters thick exposed on Yakima Ridge in Sec. 36, T13N, R23E; magnetic polarity predominantly reverse; potassium/argon age about 15 million years; maximum thickness of member about 70 meters.
- Te1 ELLENSBURG (QUINCY) INTERBED -- Rare, thin lenses of light-colored siliceous siltstone, chert, and petrified wood, occasionally baked to a brick-red color by overlying Priest Rapids basalt; maximum thickness about 3 meters.
- Tfu FRENCHMAN SPRINGS -- Six or possibly more flows of dark grey, aphyric to porphyritic basalt; undifferentiated where not mapped in detail; porphyritic flows are commonly diktytaxitic and contain from 1-7% plagioclase glomerophenocrysts up to 5 centimeters long; diktytaxitic flows weather to rusty-brown

color; aphyric flows are apparently sandwiched between top (Roza (?) Member) and bottom porphyritic unit; volume of phenocrysts is not constant laterally or vertically in porphyritic flows and may grade locally into aphyric zones; colonnade and entablature are variable, but well exposed in the cliffs east of Juniper Springs; a siliceous interbed lies between upper porphyritic and aphyric flows in outcrops too small to map; member overlies interbed (Ellensburg) or Grande Ronde Basalt; magnetic polarity normal; maximum thickness of member about 170 meters(?).

Te1 ELLENSBURG (VANTAGE) SANDSTONE INTERBED -- Discontinuous unit of white to brown, coarse- to fine-grained feldspathic sandstone with conspicuous flakes of muscovite and biotite; sandstone may or may not be well indurated; overlies Grande Ronde Basalt; maximum thickness about 30 meters.

Tsb, GRANDE RONDE BASALT -- At least 13 flows of grey to black
 Ts, generally aphyric basalt; more complete descriptions are given
 Tsu in stratigraphic section, Plate 2; undifferentiated where not mapped in great detail; formation was mapped in two units subdivided by a chemical-stratigraphic horizon, the "MgO Horizon;" the unit above this break (Sentinel Bluffs, Tsb) has a thick basal flow with a 10-15 meters thick flow top breccia; the unit below the MgO Horizon (Schwana, Ts) has a thick uppermost flow named the Umtanum flow (Tsu) with a conspicuous flow-top breccia locally over 35 meters thick; flows are cut by joints and shear zones of tectonic origin on north face of eastern Umtanum Ridge; flows locally overturned west of Priest Rapids Dam; bottom of section not exposed; all exposed flows have normal polarity, maximum exposed thickness at least 510 meters.

DISTRIBUTION

Number of
Copies

10	<u>BATTELLE-OFFICE OF NUCLEAR WASTE ISOLATION</u> S. J. Basham P. L. Hofmann R. J. Hall W. E. Newcomb W. M. Hewitt Library (5)
1	<u>CALIFORNIA ENERGY RESOURCES CONSERVATION AND DEVELOPMENT COMMISSION</u> E. Varanini
2	<u>CENTRAL WASHINGTON UNIVERSITY</u> Department of Geology Library
2	<u>EASTERN WASHINGTON UNIVERSITY</u> Department of Geology Library
5	<u>GEOLOGY OVERVIEW COMMITTEE</u> T. Livingston I. Remson H. Ross D. A. Swanson W. S. Twenhofel
6	<u>HYDROLOGY OVERVIEW COMMITTEE</u> P. Domenico R. A. Freeze P. M. Grimstad S. P. Newman F. L. Parker J. Pearson
2	<u>IDAHO BUREAU OF MINES AND GEOLOGY</u> M. M. Miller Library
1	<u>KAISER ENGINEERS INC.</u> J. S. Ritchie

Number of
Copies

1	<u>LAWRENCE LIVERMORE LABORATORY</u> L. D. Ramspott
11	<u>LOS ALAMOS SCIENTIFIC LABORATORY</u> F. E. Goff (10) K. Wolfsberg
4	<u>NATIONAL ACADEMY OF SCIENCES</u> W. E. Berg D. Daley J. Pomeroy S. Stuen
16	<u>NATIONAL ACADEMY OF SCIENCES - COMMITTEE ON RADIOACTIVE WASTE MANAGEMENT</u> M. Baram S. N. Davis E. L. Draper P. W. Durbin J. T. Edsall M. Eisenbud J. A. Fay J. C. Frye H. L. James R. E. Kasperson K. B. Krauskopf T. R. LaPorte F. L. Parker T. Pigford R. Roy E. Wenk, Jr.
1	<u>NORTHWEST ENERGY SERVICES CO.</u> J. Kearns
1	<u>OREGON DEPARTMENT OF ENERGY</u> L. D. Frank
1	<u>OREGON STATE DEPARTMENT OF GEOLOGY AND MINERAL INDUSTRIES</u> J. D. Beaulieu
2	<u>OREGON STATE UNIVERSITY</u> Department of Geology Library

Number of
Copies

4	<u>PACIFIC NORTHWEST LABORATORY</u> T. D. Chikalla J. R. Raymond S. L. Stein Library
6	<u>ROCK MECHANICS OVERVIEW COMMITTEE</u> R. Bieniawski W. Blake J. W. Corwine W. Duvall W. Hustrulid J. Russell
8	<u>SANDIA LABORATORIES</u> E. H. Beckner L. R. Hill R. C. Lincoln M. Reade S. Sinnock A. E. Stephenson L. D. Tyler W. D. Weart
1	<u>SOUTH CAROLINA GEOLOGICAL SOCIETY</u> N. K. Olson
1	<u>STATE OF IDAHO GOVERNOR'S OFFICE</u> C. Jones
1	<u>STATE OF OREGON GOVERNOR'S OFFICE</u> K. Woods
1	<u>STATE OF UTAH DIVISION OF WATER RIGHTS</u> H. D. Donaldson
1	<u>STATE OF WASHINGTON GOVERNOR'S OFFICE</u> J. Wood

Number of
Copies

1	<u>SWEDISH NUCLEAR FUEL SUPPLY COMPANY (KBS)</u> L. B. Nilsson
4	<u>U.S. ARMY CORPS OF ENGINEERS</u> Seattle District Geologist Seattle District Librarian Walla Walla District Geologist Walla Walla District Librarian
1	<u>U.S. ARMY YAKIMA FIRING CENTER</u> W. R. Dietderich
1	<u>U.S. BUREAU OF LAND MANAGEMENT</u> R. D. Scherer
2	<u>U.S. BUREAU OF RECLAMATION</u> B. H. Carter D. Newmann
2	<u>U.S. DEPARTMENT OF ENERGY-ALBUQUERQUE OPERATIONS OFFICE</u> D. T. Schueler
5	<u>U.S. DEPARTMENT OF ENERGY-COLUMBUS PROGRAM OFFICE</u> J. O. Neff
4	<u>U.S. DEPARTMENT OF ENERGY-HEADQUARTERS</u> C. R. Cooley C. H. George C. A. Heath D. L. Vieth
1	<u>U.S. DEPARTMENT OF ENERGY-NEVADA OPERATIONS OFFICE</u> R. M. Nelson
2	<u>U.S. DEPARTMENT OF ENERGY-PUBLIC READING ROOMS</u> Richland, Washington Seattle, Washington

Number of
Copies

6	<u>U.S. DEPARTMENT OF ENERGY-RICHLAND OPERATIONS OFFICE</u> T. A. Bauman R. B. Goranson A. G. Lassila B. L. Nicoll D. J. Squires F. R. Standerfer
9	<u>U.S. GEOLOGICAL SURVEY</u> C. Collier G. D. DeBuchananne M. H. Hait T. Hait W. Hays R. Schneider R. Schuster P. R. Steven T. L. Wright
9	<u>U.S. NUCLEAR REGULATORY COMMISSION</u> M. J. Bell R. Boyle J. O. Bunting, Jr. L. Hartung P. S. Justus J. C. Malaro J. B. Martin E. P. Regnier L. D. White
2	<u>UNIVERSITY OF IDAHO</u> Department of Geology Library
3	<u>UNIVERSITY OF OREGON</u> G. G. Goles Department of Geology Library
4	<u>UNIVERSITY OF WASHINGTON</u> S. D. Malone S. W. Smith Department of Geology Library

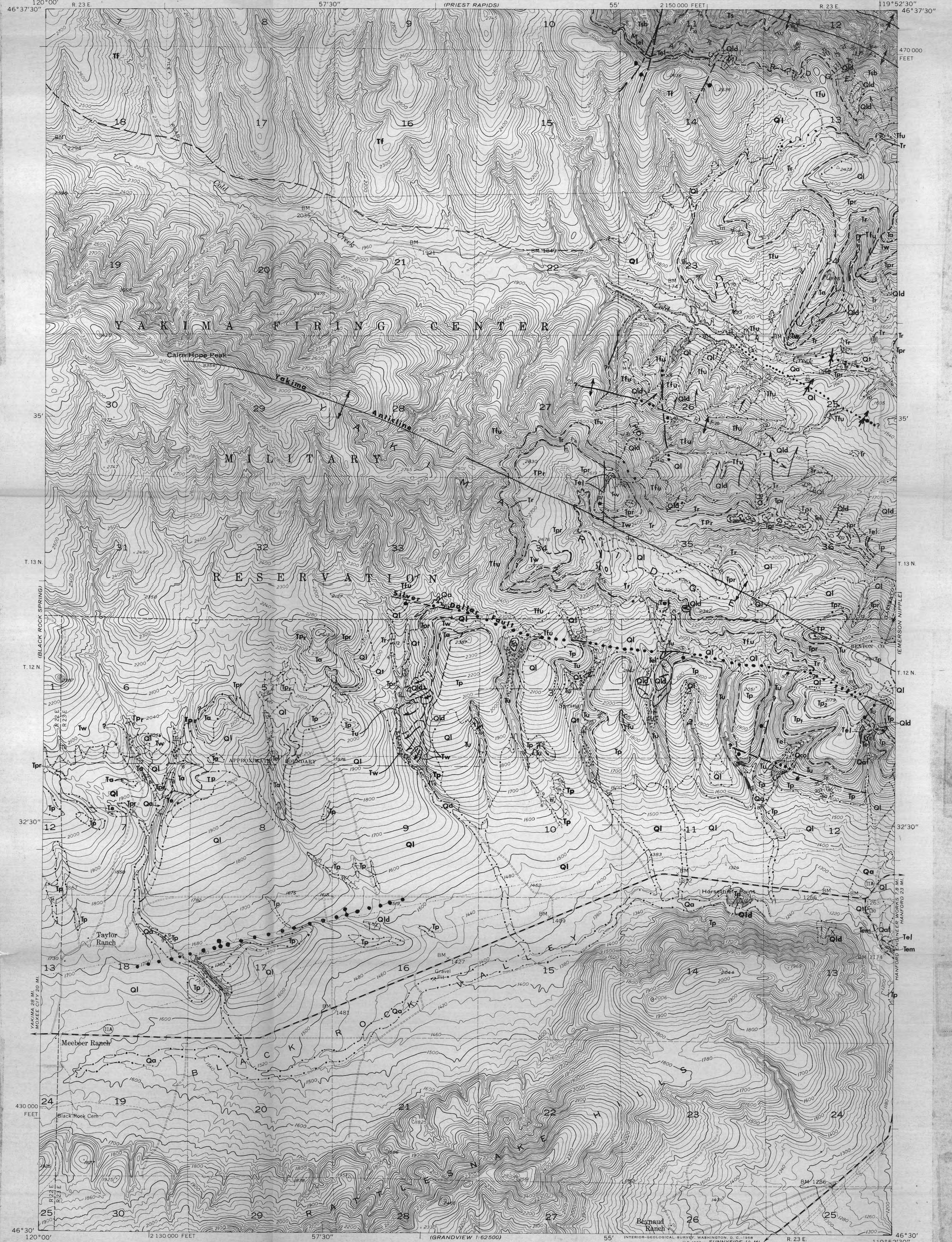
Number of
Copies

1	<u>WASHINGTON PUBLIC POWER SUPPLY SYSTEM, INC.</u> D. D. Tillson
1	<u>WASHINGTON STATE DEPARTMENT OF ECOLOGY</u> Library
1	<u>WASHINGTON STATE DEPARTMENT OF NATURAL RESOURCES</u> Library
2	<u>WASHINGTON STATE UNIVERSITY</u> Department of Geology Library
1	<u>A. C. WATERS</u>
2	<u>WESTERN WASHINGTON UNIVERSITY</u> Department of Geology Library
2	<u>WESTINGHOUSE WIPP PROJECT</u> R. C. Mairson
29	<u>ROCKWELL HANFORD OPERATIONS</u> D. J. Brown D. J. Cockeram T. A. Curran R. A. Deju F. A. DeLuca R. J. Gimera R. N. Gurley M. J. Smith Basalt Waste Isolation Project Library (15) Document Control (4) Records Retention Center (2)

UNITED STATES
DEPARTMENT OF THE INTERIOR
GEOLOGICAL SURVEY

UNITED STATES
DEPARTMENT OF THE ARMY
CORPS OF ENGINEERS

CAIRN HOPE PEAK QUADRANGLE
WASHINGTON
7.5 MINUTE SERIES (TOPOGRAPHIC)
SW1/4 PRIEST RAPIDS 17 QUADRANGLE



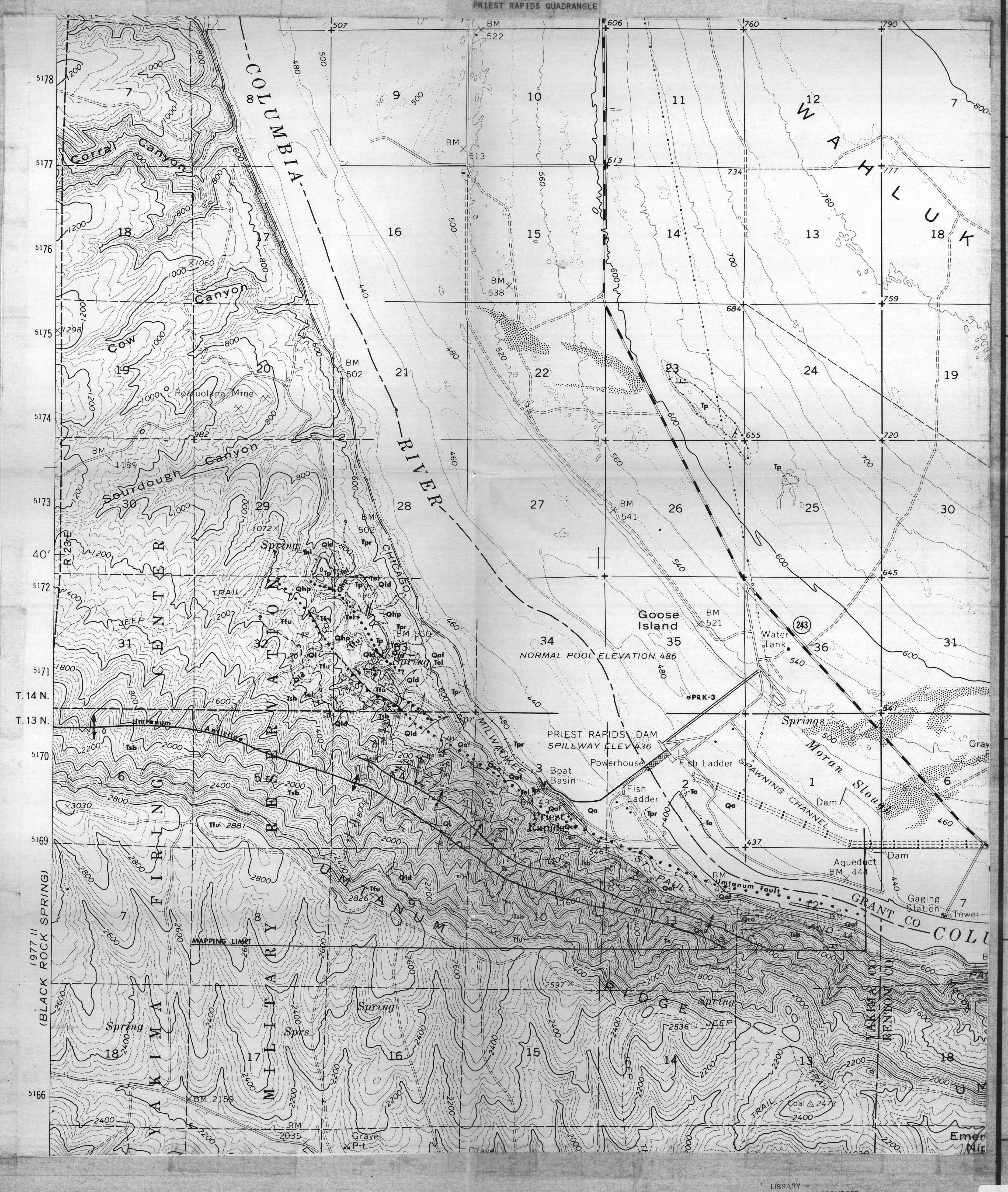
Mapped by the Army Map Service
Published for civil use by the Geological Survey
Control by USGS, USC&GS, and U.S. Bureau of Reclamation
Topography by USGS from aerial photographs by multiplex methods
Aerial photographs taken 1948
Polyconic projection, 1927 North American datum
10,000-foot grid based on Washington coordinate system,
south zone
1000-meter Universal Transverse Mercator grid ticks,
zone 11, shown in blue
Dashed land lines indicate approximate locations
Unchecked elevations are shown in brown

SCALE 1:24,000
CONTOUR INTERVAL 20 FEET
DATUM IS MEAN SEA LEVEL

ROAD CLASSIFICATION
Medium duty — Light duty
Unimproved dirt —
State Route

CAIRN HOPE PEAK, WASH.
SW1/4 PRIEST RAPIDS 17 QUADRANGLE
N4630—W11952.5/7.5
1948

FOR SALE BY U.S. GEOLOGICAL SURVEY, DENVER 2, COLORADO OR WASHINGTON 25, D. C.



LIBRARY
DEPARTMENT OF NATURAL RESOURCES
GEOLOGICAL AND ENVIRONMENTAL SURVEY
OLYMPIA, WASHINGTON 98504

**GEOLOGIC MAP OF EASTERN UMTANUM RIDGE
AND YAKIMA RIDGE SOUTH-CENTRAL WASHINGTON**

BY FRASER GOFF

POCKET PART 1 OF 2
RHO-BWI-C-21

QEI76
B4
6612p
1981
copy 2
Plate 1